Investigation of a valveless pulse-combustor

Everson, G

INVESTIGATION OF A VALVELESS PULSE-COMBUSTOR

M.Sc. Thesis

G. Everson - 1971

SUMMARY

A gas-fired pulse combustor based on a design by F.H. Reynst has been built and tested to determine the characteristics of this particular type of combustor and the form of combustion instability on which the operation of the combustor depends.

These tests have established (a) that the chamber always operates at a frequency much lower than its Helmholtz frequency, (b) that the frequency depends on the rate at which fuel is supplied to the combustor, and (c) that there is a linear relationship between frequency and fuel flow.

An analysis of the induction process has confirmed that the principal cause of the induction is the contraction (due to cooling) of the gases remaining in the combustion chamber at the end of the exhaust period. Some form of wall and base cooling is therefore essential to the operation of a gas-fired combustor of the Reynst type.

Finally, as a result of this investigation, it has been concluded that the form of instability in a Reynst type combustor is of the fluid dynamic type of combustion chamber instability.

CONTENTS

Continued ...

Contents Continued

Continued ...

Contents Continued

1. INTRODUCTION

A survey of combustion research literature reveals that there is a considerable interest in the phenomenon of combustion instability. Two main reasons for this interest are apparent. The first and perhaps the most important of these is the need to understand the various forms of instability in order to eliminate, possibly at the design stage, the unwanted combustion oscillations that frequently occur in steady-flow combustors. The other reason, which is the one that concerns this investigation, is that pulsating combustion appears to offer certain advantages over steady-flow combustion for applications in the fields of industrial and domestic heating; these advantages are summarised below.

1. High combustion intensity - rates as high as 44.5 Mw/m^3 are reported in the literature.
2. Forced, induced, or natural draught is not required - pulse combustors can operate against a back pressure and draw in combustion air.
3. The pulsating nature of the hot gas flow from a pulse combustor gives rise to heat transfer rates that are higher than those normally found in comparable steady-flow combustors.

The combustor that is the subje ct of this investigation is based on a design by F.H. Reynst[7]. An unusual feature of this design is that the combustion chamber has

only one opening which serves as both inlet and exhaust port, the exhaust gas and fresh charge flowing alternately through this opening; to the best of the authors knowledge all other pulse combustors designed to date have separate inlet and exhaust ports.

A problem common to pulse combustors is that of exhaust gas blowing out through the inlet port. To stop this 'blow back', the inlet may be fitted with either a mechanical valve or an aerodynamic valve, combustors employing the latter are frequently referred to as 'valveless' combustors.

Mechanical valves usually take the form of thin reeds or diaphragms which respond to combustion chamber pressure in such a way that when the pressure begins to rise due to the onset of combustion, the valve closes, thereby preventing exhaust gas escaping through the inlet. Valves of this type are quite efficient when new but they tend to have rather short working lives and hence require regular inspection and replacement.

Aerodynamic valves are essentially ducts which offer a greater resistance to flow in the reverse direction than in the forward direction. Since they contain no moving parts their useful life is virtually indefinite, however, they cannot prevent blow-back completely and when used on conventional pulse combustors (those that employ separate combustion chamber inlet and exhaust ports) there is evidence to suggest that intake silencing becomes

difficult, if not impossible.

In the case of the Reynst combustor which is of the valveless type, the prevention of blow-back is achieved by arranging the combustion chamber and exhaust pipe in the form of an ejector (Figure 3.2) so that during the exhaust period air is drawn in through the intake by the ejector action. Freedom from blow-back combined with the absence of mechanical valves makes the Reynst design particularly suitable for application as a domestic heater. However, at present there is not sufficient information available to enable heating units based on the Reynst combustor to be designed.

The aim of this investigation is to acquire some data on the design and operation of a Reynst combustor and to determine the form of instability on which the operation of the combustor depends.

2. REVIEW OF THE FIELD

2.1 Pulsating-combustion Heaters

Although a considerable amount of work has been done on pulsating combustion the application of pulsating combustion to heating appliances is relatively new. A number of attempts are now being made to develop pulsating-combustion heaters[1,2,3] but only one unit is at present commercially available. This unit is the "Pulsamatic" gas-fired water heater developed by Lucas Rotax of Canada which is described in a paper by Alebon, Lee and Gellar[4].

Patent literature contains many examples of pulsating combustor designs, but just how many of these designs actually work is difficult to determine. One design which has been developed to the stage where it could be applied is due to Huber[5]. This unit is intended to be used as a hot gas generator for such applications as engine heating (for starting in extremely cold climates) and an investigation of a combustor based on Huber's design has been carried out by Sampath[6].

Porter[8] has studied a Reynst type combustor and found that (i) for a given chamber diameter, pulsating combustion only occurred when the chamber length and port diameter were within certain limits, (ii) the shape of the cross-section of the chamber was not important, (iii) enriching the combustion air with oxygen stopped pulsating combustion, and (iv) the pulsation frequency was lower than the Helmholtz frequency*

* Helmholtz combustor - Figure 2.1

by a factor of three.

Other interesting papers on pulsating combustion are given in the bibliography.

2.2 Classification of Pulse Combustors

Pulse combustors can, in general, be classified as Helmholtz type or Schmidt type; in practice the division is not always clear[2]. Details of these two basic types are as follows:-

Helmholtz Combustor

Figure 2.1 shows the main features of a Helmholtz type combustor which are: a short inlet pipe (1), (sometimes fitted with mechanical valves at its upstream end), the combustion chamber (2), and an exhaust pipe (3). The operating frequency of this type of combustor depends mainly on the acoustic properties of the air inlet pipe - combustion chamber combination, which functions as a Helmholtz resonator. Ideally the length of the exhaust pipe should be such that its quarter wave frequency is the same as the Helmholtz frequency of the chamber.

Schmidt Combustor

The Schmidt type of combustor shown in Figure 2.2 has the same form of inlet (1) as the Helmholtz combustor but the exhaust pipe (3) of the Schmidt combustor is the same diameter as the combustion chamber (2). The operating frequency of a Schmidt combustor is determined by the length

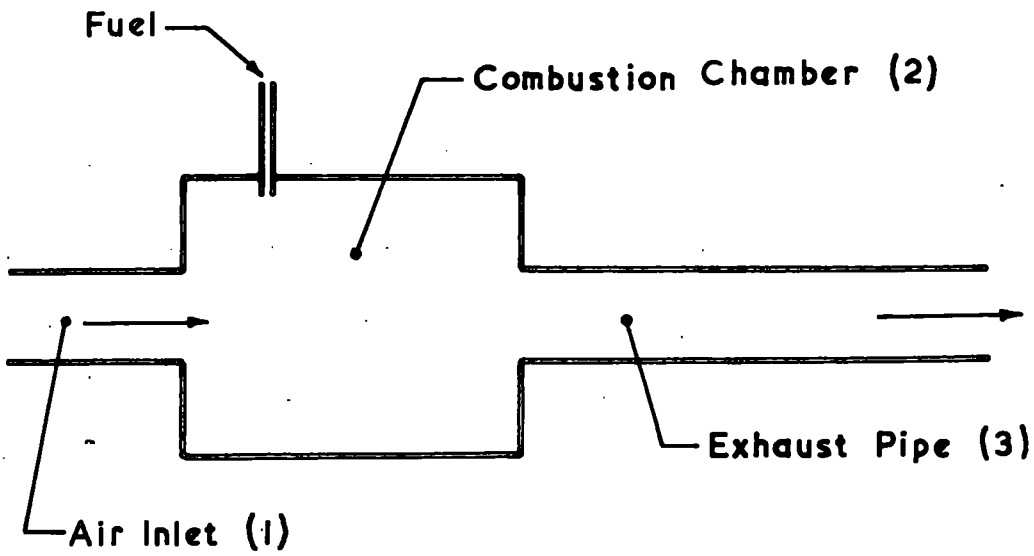

Figure 2·1 — Helmholtz Combustor

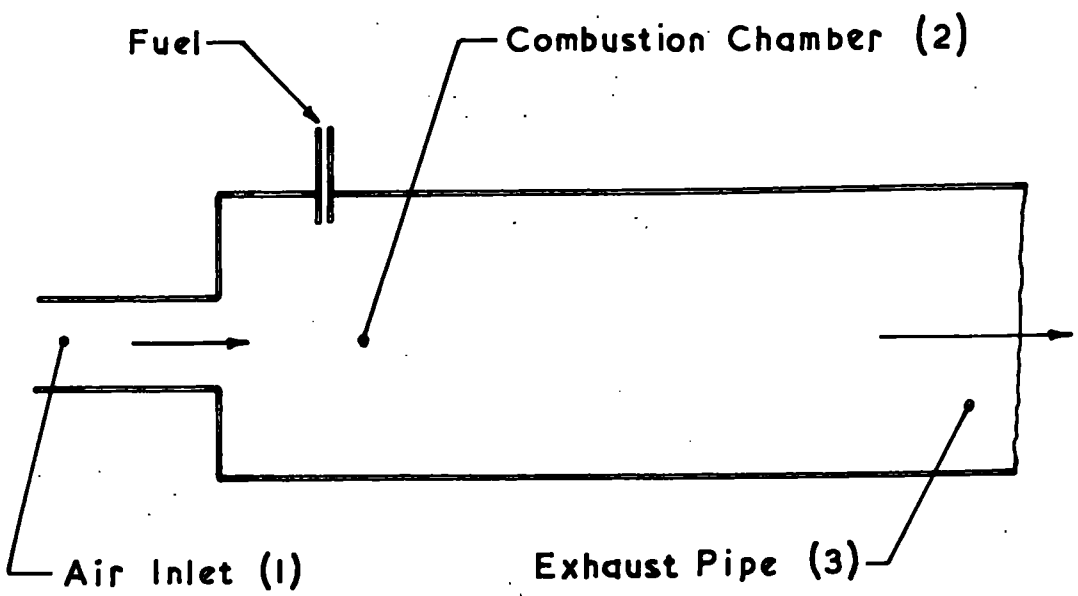

Figure 2·2 — Schmidt Combustor

of the gas column between the open and closed ends of the main tube. This gas column oscillates on a quarter wave mode having a pressure antinode at the closed end of the tube.

Classification of Reynst Combustor

On the grounds of chamber geometry the Reynst combustor could be classified as Helmholtz type. The operating characteristics are however quite different to those of the true Helmholtz combustor in that the frequency of pulsation is not determined by the Helmholtz frequency of the combustor, indeed the frequency can be varied over a considerable range simply by regulating the fuel flow[7].

2.3 Noise from Pulse Combustors

A characteristic of pulsating combustion is the emission of intense sound and this sound emission is one of the main problems facing designers of pulsating combustion heaters. Some idea of the noise level of a pulsating combustor is given by Reynst[7] who claimed that on occasions his largest combustors could be heard from a distance of several miles!

It is therefore essential for pulsating combustors intended for use as industrial or domestic heaters, to be fitted with highly efficient silencers, both on the exhaust and the air intake.

Research into the problem of silencing pulsating combustors has been carried out by Reay[3] who claims that a noise level of about 120 dB from an unsilenced 58.6 kW

combustor was reduced to about 80 dB by means of all-absorptive mufflers fitted to the inlet and exhaust. However, according to Reay further reduction would be impracticable since at the 80 dB level the noise was emanating from many different parts of the combustor.

In the domestic heating field Gellar, Lee and Mitchell[1] studied the problem of silencing a 29.3 kW pulsating combustion heater and as a result of their work the noise level of the heater was reduced to about 62 dB.

2.4 Classification of Combustion Instability

In the literature on combustion instability the classification of combustion instability according to type has been attempted by several authors and two schemes of classification, one by Putnam[9] and another by Barrére and Williams[10] are of particular interest.

2.4.1 Putnam's Classification of Instabilities

Putnam defines three types of instability. These are:

(1) System Instability

Instability of this type involves the entire combustion system, combustion chamber-fuel supply lines etc. "Chugging" of rocket motors is an example of system instability.

(2) Acoustic Instability

In the case of acoustic instability the frequency of the oscillations is closely related to the acoustical properties of the combustor. With this type of instability various modes of oscillation are possible, such as

axial mode, tangential mode, radial mode and combinations of these modes. "Singing Flames" and "Gauge Tones" are well known cases of acoustic instability.

(3) Transition Instability

This type of instability is associated with periodic changes in the combustion pattern. For example, under certain conditions two alternative flow patterns may be possible and the system may "hunt" between these two patterns. If in addition the two alternative flow patterns produce different rates of heat release then the tendency to "hunt" may turn into a definite heat driven oscillation.

2.4.2 Barrére and Williams Classification Scheme

The classification scheme adopted by Barrére and Williams has three main classes, these are:-

(1) Combustion chamber instabilities,

(2) System instabilities,

(3) Intrinsic instabilities.

Combustion Chamber Instabilities

Combustion chamber instabilities are divided into three types, (a) acoustic instability, (b) fluid dynamic instability and (c) shock instability.

The acoustic instability and fluid dynamic instability of this scheme are, therefore, equivalent to the acoustic and transition instabilities respectively of Putnam's scheme.

Shock instability is due to the presence of finite amplitude shock or detonation waves in the combustion chamber.

System Instabilities

This class of instability is identical to the system instability class of Putnam.

Intrinsic Instabilities

Intrinsic instabilities are due to the nature of the reactants themselves, for example, hetrogeneous solid propellants can show periodic local burning due to their hetrogeneous structure.

From a comparison of the above classification schemes it is evident that the scheme of Barrere and Williams is the most comprehensive. If as a result of this investigation any conclusion can be reached concerning the form of instability in a Reynst combustor the classification will be made in accordance with the Barrére and Williams scheme.

3. DEVELOPMENT OF COMBUSTOR DESIGN

3.1 Historical

Reynst's work on pulsating combustion began in the 1930's with the invention of a valveless pulsating-combustion chamber for which he obtained a patent (Swiss Patent 196312) in 1938; a schematic diagram of this combustor is shown in Figure 3.1 . In his papers on pulsating combustion, which have been collected and edited by Thring[7], Reynst discusses many applications for his combustor ranging from water heating to boundary layer propulsion of aircraft, however, in developing his combustor Reynst appears to have been mainly interested in its use as a heating device. A diagram of a liquid-fueled pulsating-combustion heater designed by Reynst is shown in Figure 3.2, the principal differences between this design and that of Figure 3.1 being (i) the addition of a diffuser (exhaust pipe) and (ii) provision of a means of increasing the chamber volume for starting. The combustor shown in Figure 3.2 represents one of the latest of Reynst's designs.

3.2 Principle of Operation of a Reynst Combustor

The following account of the operation of the combustor is based on Reynst's own explanation.

To start the combustor (shown in Figure 3.1), gas is fed into the combustion chamber (1) through a nozzle in the base of the chamber, and ignited by means of a sparking plug. This initial charge burns rapidly and the products

of combustion flow out of the combustion chamber through the single opening at the top. The gases remaining in the combustion chamber at the end of the exhaust period are cooled by contact with the water-cooled walls of the chamber. As a result of the cooling, the gases contract and the pressure falls below atmospheric, thereby inducing a fresh charge of air to enter the chamber. The large internal nozzle (2) serves to maintain the jet formation of the inflowing air so that the air penetrates deep into the combustion chamber before spreading out and mixing with the gas still flowing in through the gas nozzle. Residual hot gas or flame from the previous combustion period ignites the fresh charge and the process begins again. In this way a cyclic combustion process is set in operation, the single opening in the chamber acting as exhaust port and inlet alternately.

Once the process has been started, gas is supplied to a mixing chamber (3) from where it is drawn into the combustion chamber with the air during the induction period. The gas to the nozzle in the base is then turned off and the chamber continues to operate on an inducted gas-air mixture; Reynst claims that the combustion is more complete when the gas is inducted with the air.

The frequency for a chamber of the size of that shown in Figure 3.1 would be of the order of 25 Hz.

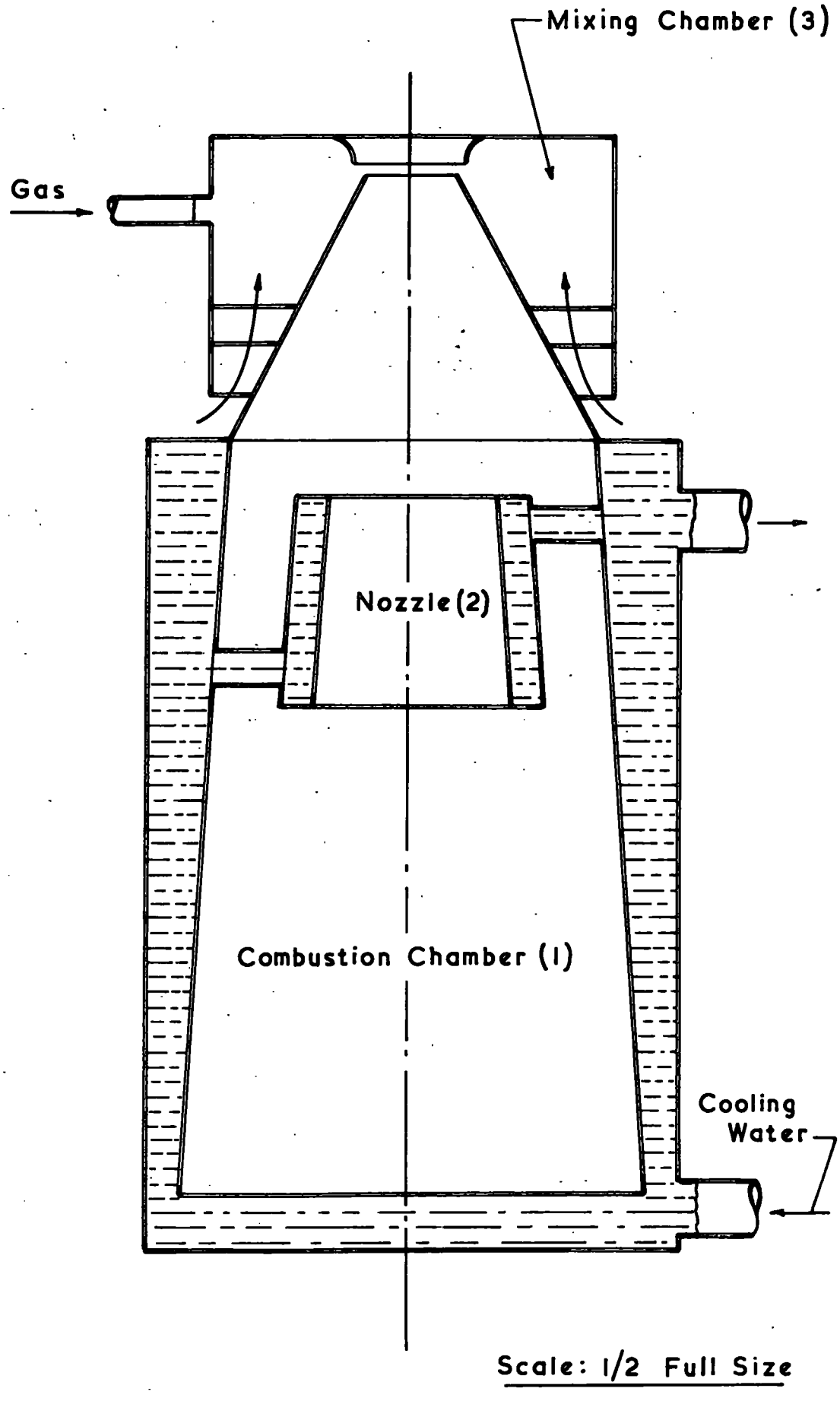

Figure 3·1 Basic Reynst Combustor.

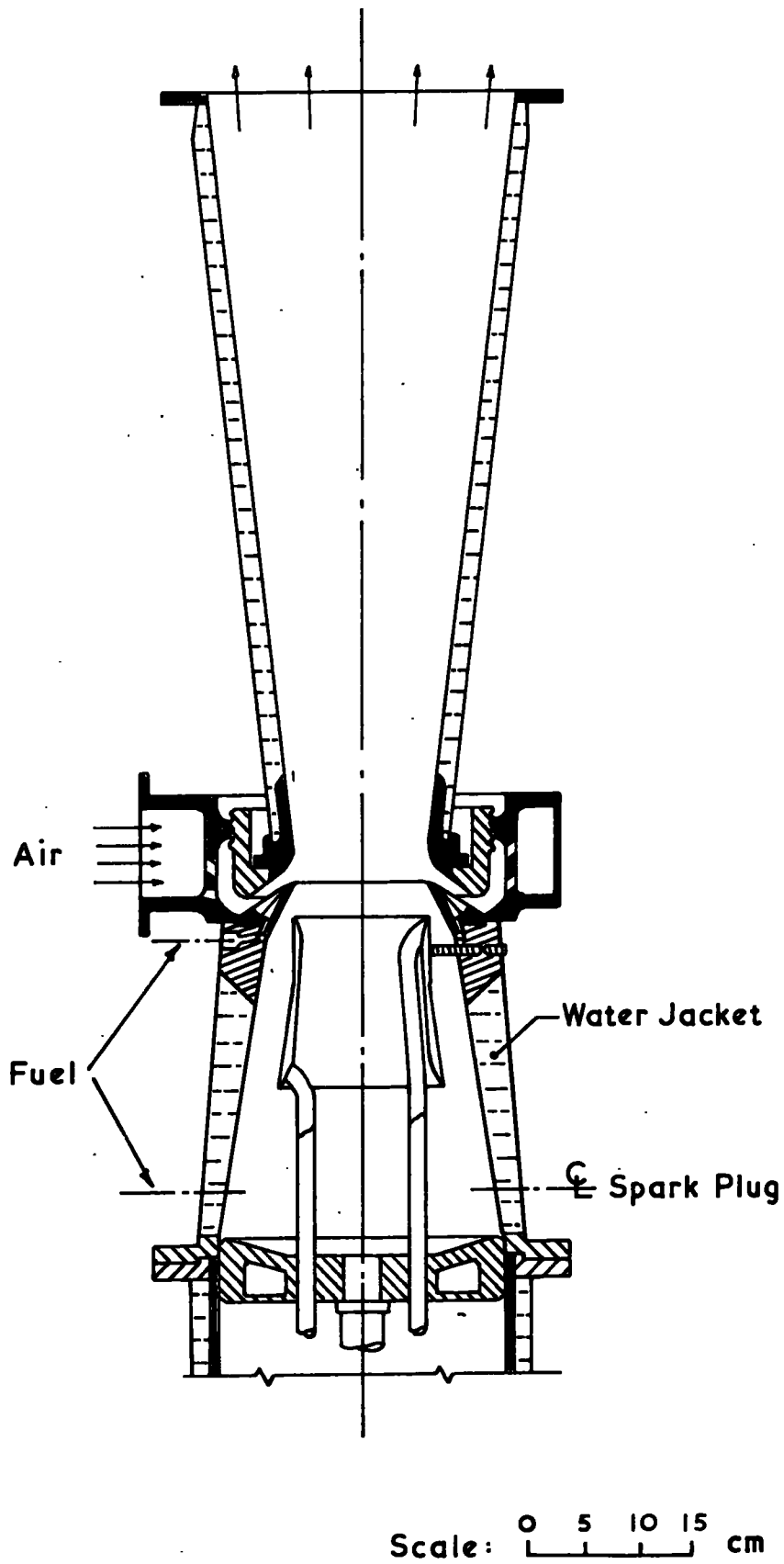

Figure 3·2 Reynst Combustor—Later Design.

3.3 Design of experimental combustors

Although Reynst offers an explanation of the principle of operation of his combustor, he does not give any quantitative experimental or theoretical basis for combustor design. Consequently, in constructing a combustor for the purposes of this investigation, it was necessary to resort to cut and try methods, and as a result, three combustors were built before a satisfactory design was obtained. An account of this development work follows.

3.4 Combustor I

A cross-section of Combustor I is shown in Figure 3.3 The combustor was designed to burn propane gas which, for starting the combustor, was fed directly into the combustion chamber through nozzle (2). For continuous operation the propane was supplied to the gas ring (3) to be drawn into the combustor with the combustion air. A sparking plug (not shown in Figure 3.3) was used to ignite the initial charge, the plug was mounted in the base of the chamber and the high tension supply for the plug was obtained from an ignition unit of the type used in sparking plug test equipment. The diffuser (5) was mounted on three jacking screws which provided a means of adjusting the gap between the diffuser and the combustion chamber.

Combustor I was designed as a simplified version of the combustor shown in Figure 3.2, the simplification of the design being mainly for manufacturing reasons. However, the piston (Figure 3.2) which, in the Reynst combustor, was used to regulate the chamber volume for starting purposes

was not omitted in Combustor I for manufacturing reasons, but on the grounds that in a domestic water heater such a device would be unacceptable, and that it was, therefore, necessary to determine whether or not the combustor could be made to operate without it.

Tests on Combustor I

The first attempt to start the combustor failed because the initial charge could not be ignited (by means of the sparking plug). Many further attempts were made for propane pressures up to 140 kN/m^2 gauge and for propane nozzle sizes in the range 0.75 mm to 3.75 mm diameter but without success. The failure to ignite the initial charge was thought to be due to inadequate mixing of the gas and air. To improve mixing, the purging air was turned on at a reduced pressure; this technique proved partly successful in that ignition of the initial charge was achieved for each combination of gas nozzle diameter and gas pressure previously tried. In no case, however, did pulsating combustion follow the burning of the initial charge. During these tests it was noticed that the sound from the spark increased steadily in pitch as gas was admitted to the combustion chamber and with practice it became possible to predict quite reliably the instant when ignition was about to occur.

Although the combustor would not operate with the propane fed directly into the chamber it was considered possible that the chamber would operate with the propane

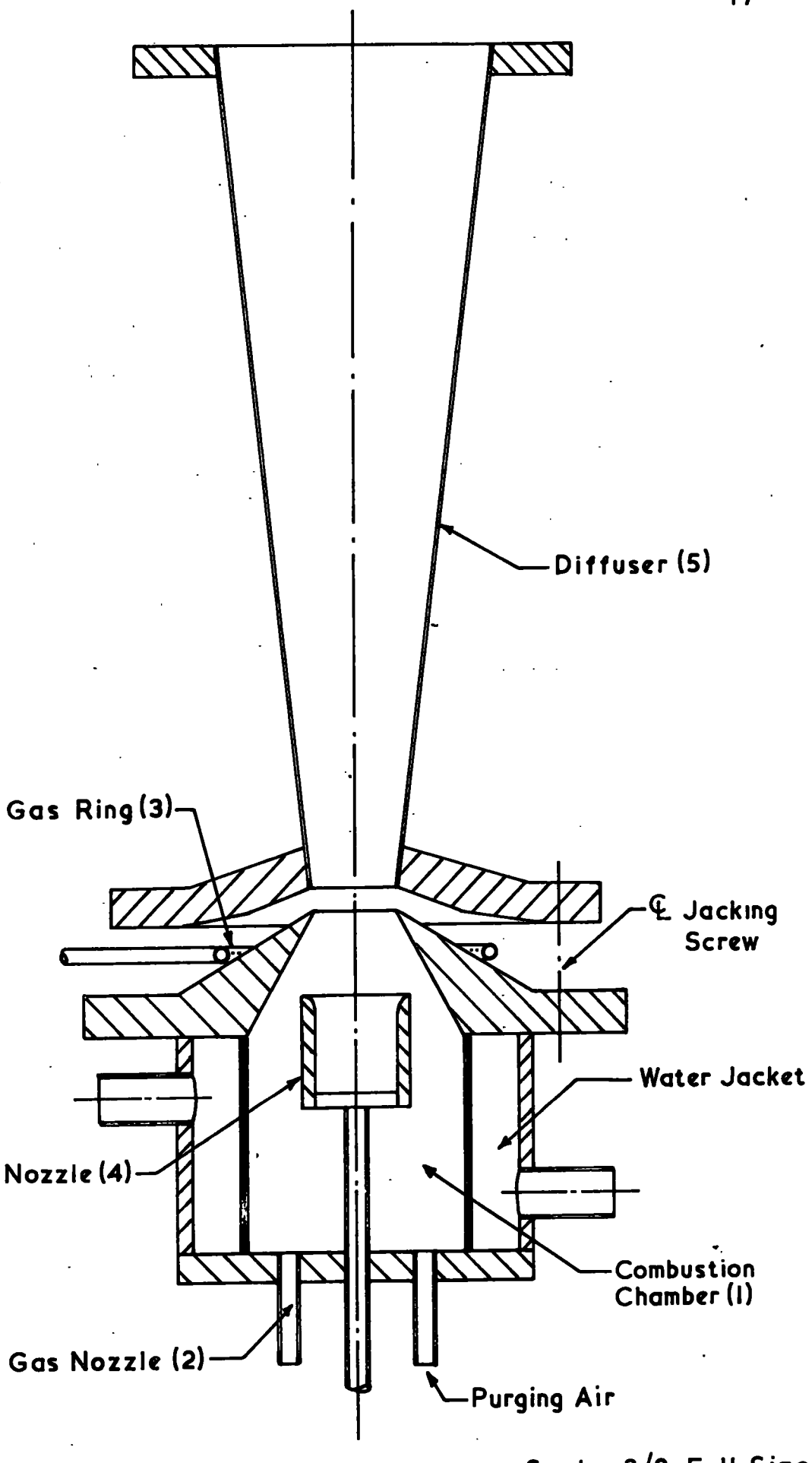

Figure 3·3 Combustor I

inducted with the combustion air and that the process might be started using the single pulse from the combustion of the initial charge.

This was tried and after a few attempts regular pulsating combustion started. The method adopted for starting the combustor was to use the sound from the spark as guide to predict ignition and to turn on the gas supply to the gas ring just before ignition was expected to occur (to turn the gas on sooner than this would have resulted in a large accumulation of gas in the diffuser). The frequency of the pulsations was very low (about 2 H_z) and the pulsations stopped if either the electrical ignition or the purging air was turned off. Since the chamber would not operate without the forced air supply this indicated that the mixture might be too rich. To weaken the mixture the gas pressure was reduced and as a result it was found that less forced air was required and the frequency increased. However, the pulses rapidly diminished in strength with reduction of gas pressure and before the stage was reached where the forced air could be turned off the pulsations ceased. Another method of reducing the mixture strength was tried, this was to increase the gap between the chamber and the diffuser to permit a greater air flow into the chamber. This gap proved to be quite critical and could only be increased by a small amount which did not have the desired effect on the operation of the chamber.

The tests on Combustor I continued, with many modifications being made to the chamber. These modifications included (a) increasing the volume of the combustor by increasing its length with extension pieces, (b) changing the chamber port diameter by fitting orifice plates over the existing port and (c) changing the position and type of gas nozzle. The attempts to secure correct operation of the combustor, however, remained unsuccessful and it was decided that a fresh start should be made with a simpler design based on the combustor shown in Figure 3.1.

3.5 Combustor II

Figure 3.4 shows a sketch of Combustor II; the positioning of the sparking plug in the chamber wall and near to the top of the chamber was based on experience gained from the work on Combustor I. It was also established by the tests on Combustor I that the best initial combustion was produced when the gas entered the chamber in a radial direction but the optimum height of the gas jet above the base of the chamber was not ascertained by these tests. The gas nozzle for Combustor II was therefore designed to meet the following requirements:-

(a) the gas to be discharged horizontally,

(b) the height of the nozzle above the base of the chamber to be adjustable,

(c) the angular position of the gas jet in relation to the sparking plug to be adjustable.

3.5.1 Water-Cooling System

Only the walls of the chamber were water-cooled, the water flowing from a "shower head" at the top of the chamber. The water was collected in a tank (not shown in Figure 3.4) below the chamber, and from the tank it was discharged into a drain. This method of water-cooling was adopted to simplify the installation of probes, pressure tappings etc., when required.

3.5.2 Tests on Combustor II

With this combustor, rapid (25 H_z) self-sustaining pulsating combustion was soon obtained. The position of the gas nozzle was found to be quite critical, the chamber would only operate with the gas entering close to the base. Gas pressure was less critical, the chamber would work at any gas pressure in the range 14 to 24 kN/m^2 gauge for a 3.18 mm diameter gas nozzle. Another gas nozzle 1.59 mm diameter was tried and this was found to give more regular pulsating combustion.

The chamber was at times difficult to start and the starting pulses were often quite strong. As a result of these strong pulses the lower part of the combustion chamber became badly distorted and although repair was possible it was not considered to be practicable since the damage was still likely to occur again. It was, therefore, decided that a new combustor should be built, similar to Combustor II but stronger and with improvements based on the experience gained from the work on Combustor II.

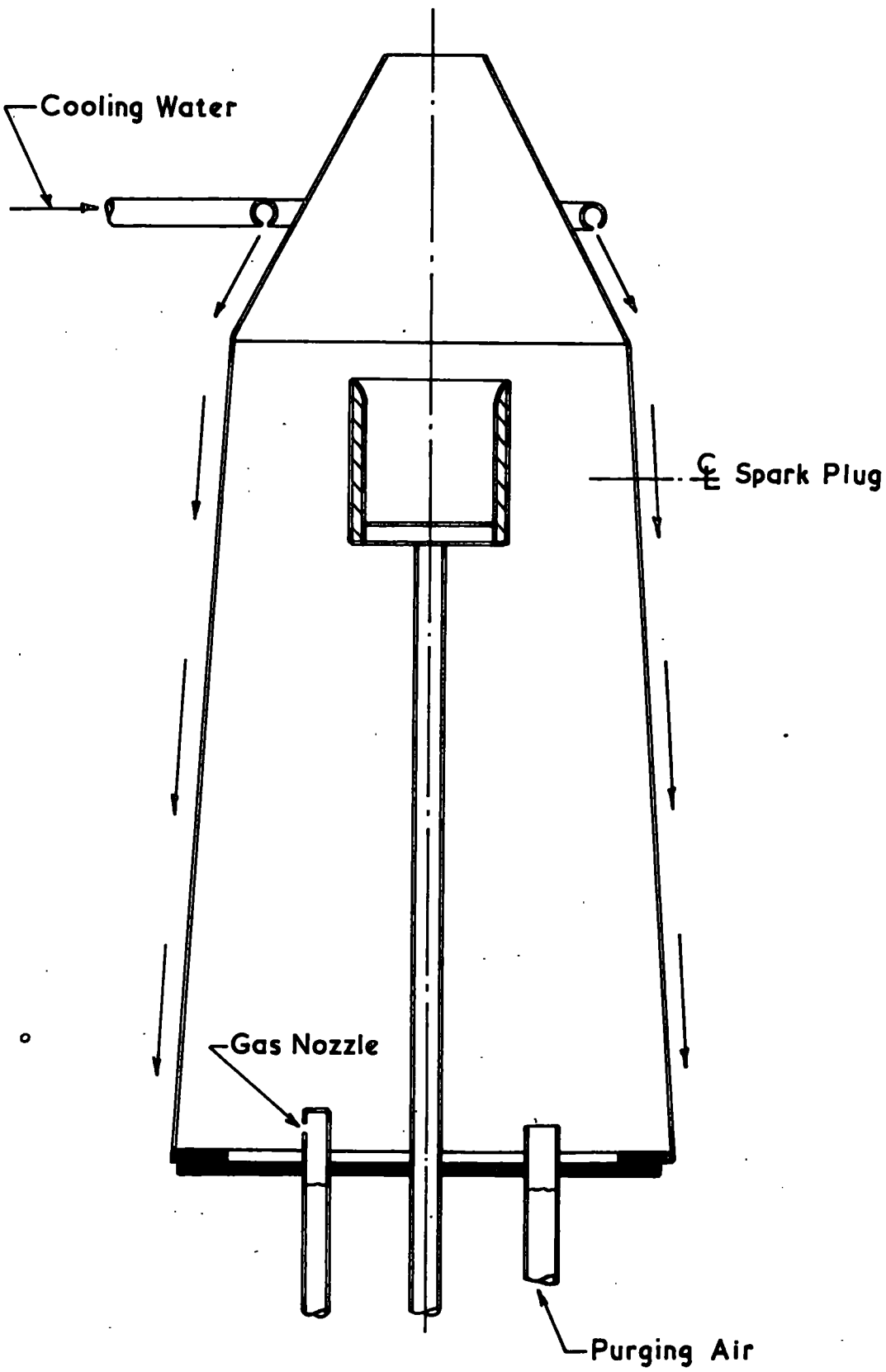

Scale: 1/2 Full Size

Figure 3·4 Combustor II

3.6 Combustor III

No difficulties were experienced in operating this combustor (Figure 3.5) with the gas entering the chamber through the nozzle (1) in the base. Starting was found to be simple and reliable and providing the condensate was drained off continuously the chamber would operate for as long as required. If the condensate was not removed then the level soon reached the gas nozzle and stopped the chamber operating.

The water-cooling system was similar to that of Combustor II but in addition the base of the chamber and the internal nozzle (2) were also water-cooled. To water-cool the base the level of the water in the collecting tank was adjusted so that the base was submerged.

A considerable amount of time was spent on attempts to operate the combustor on an inducted gas/air mixture. These attempts, however, were not successful and it was decided that this should be the subject of a later investigation. For the purposes of the present investigation, therefore, the mixing chamber was removed and the water-cooling system extended to cover the top section of the chamber. Figure 3.6 shows the modified combustor.

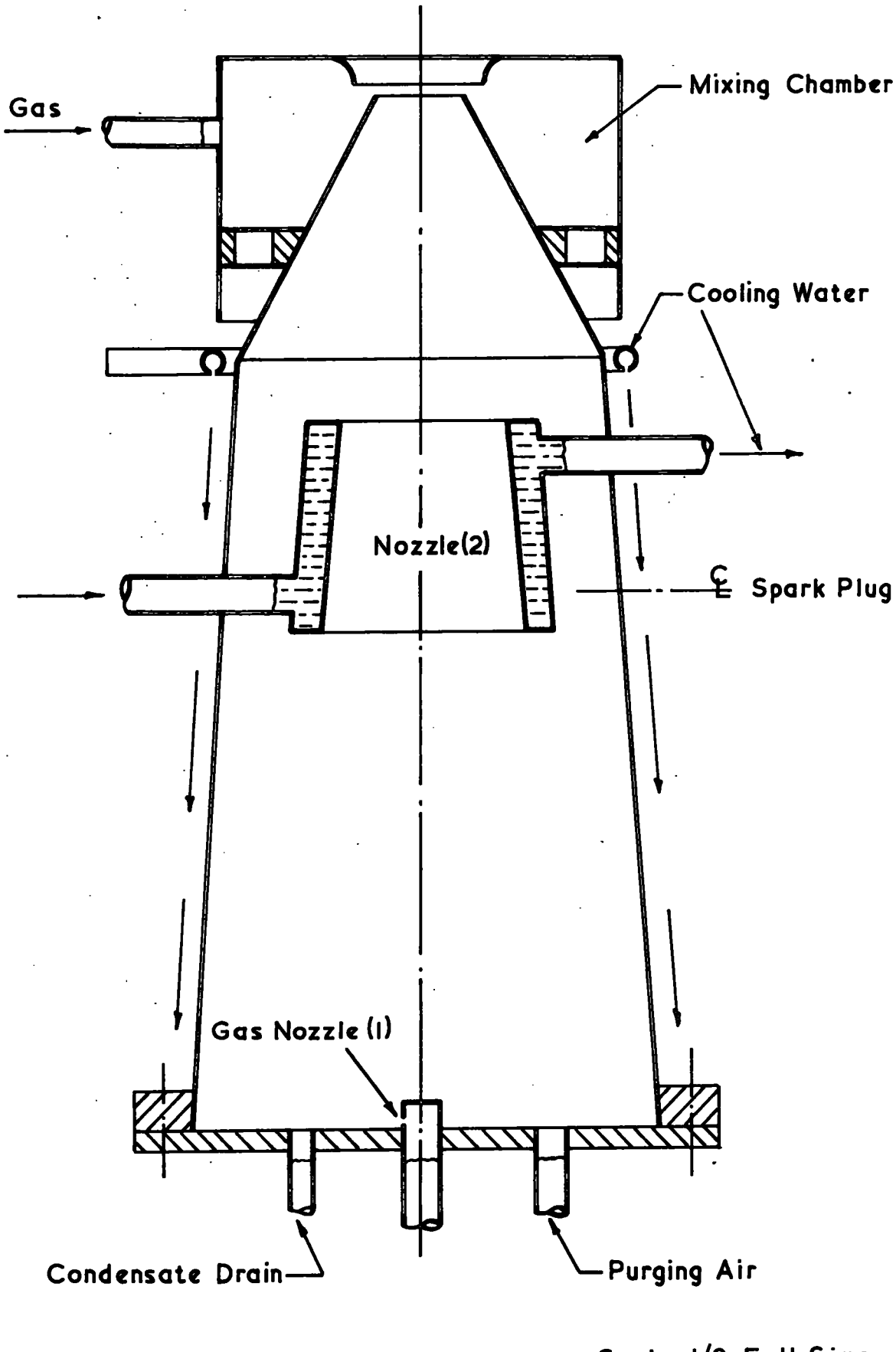

Figure 3-5 Combustor III

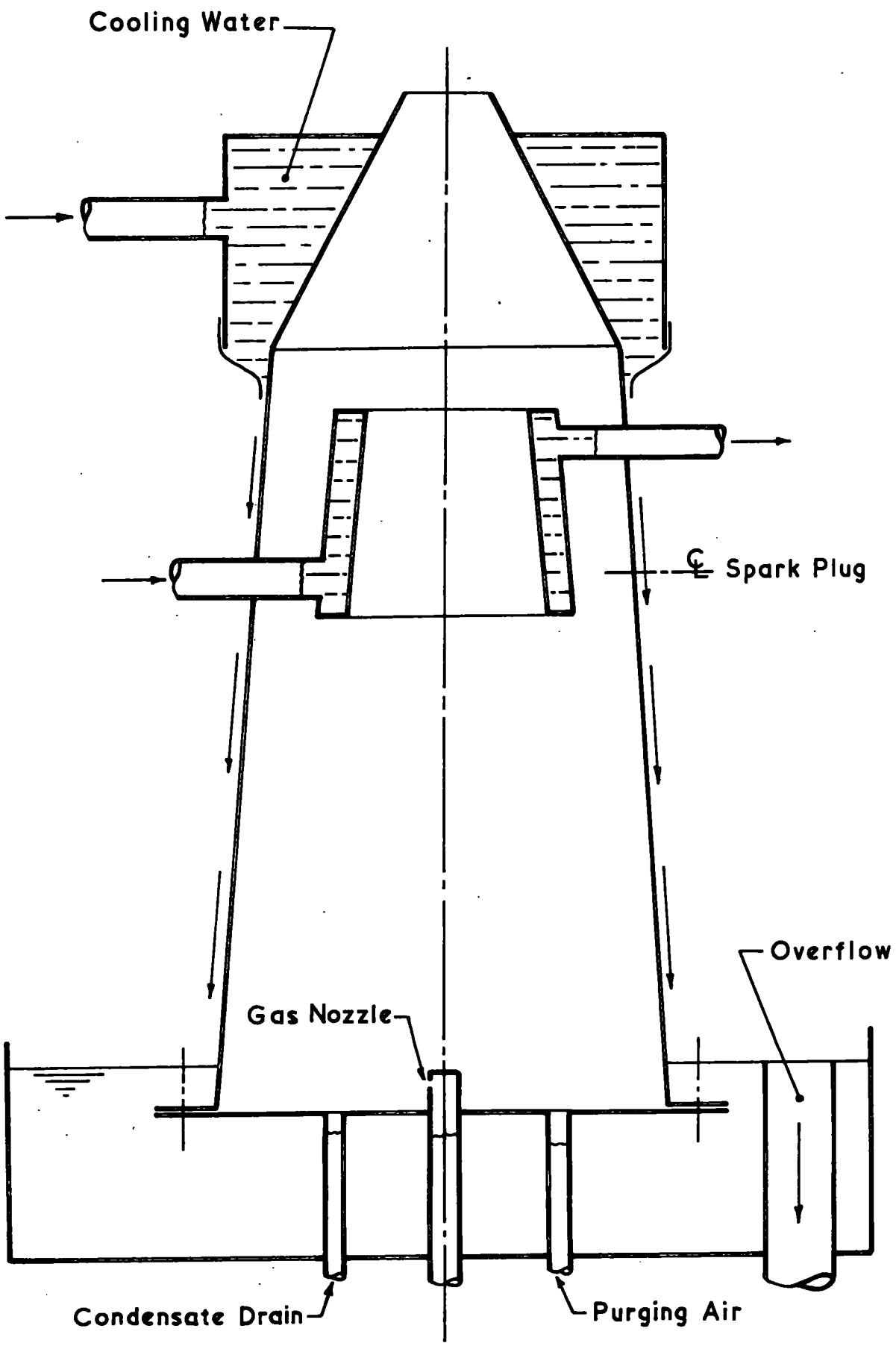

Figure 3·6 Combustor III after modifications.

4. EXPERIMENTAL METHODS

4.1 Pressure Measurements

Combustion chamber pressure was measured using two Kistler 601 A piezo-electric pressure transducers and one Bell and Howell 4-393 strain gauge pressure transducer.

The piezo-electric transducers had a range of 0-250 bar and since the maximum chamber pressure was only about 1.05 bar it was necessary to use a pre-amplifier in addition to the usual 'charge amplifier' for some measurements. Calibration of the recording system using these transducers was made difficult by the fact that the system could not record static pressures. The method used for calibrating the system consisted of applying a sudden pressure of known magnitude to the transducer and noting the deflection on the display equipment (usually an oscilloscope). In view of the uncertainty of the calibration of the piezo-electric transducers they were used only for the investigation of pressure waveform and in particular for the comparison of pressure waveforms and phase relationships, for several points along the chamber. The pressure tappings used are shown in Figure 4.1.

For accurate determination of the absolute peak chamber pressures the strain gauge transducer was used in conjunction with a U.V. recorder. Since this transducer could record static pressure the calibration of the measuring system was achieved by simply applying pressure to the transducer by means of a type of dead weight gauge tester.

The actual pressure applied was measured with a mercury manometer.

The records obtained from the U.V. recorder were also used for the determination of pulsation frequency.

4.2 Temperature Measurements

4.2.1 Cooling-water, Propane, and Air Temperatures

These temperatures were measured using copper-constantan thermocouples. The thermocouples were connected to a Honeywell multipoint chart recorder calibrated for copper-constantan thermocouples over the range 0-300^{o}F.

Figure 4.2 shows a schematic diagram of the rig, the thermocouples being indicated by T_1, T_2, T_3 etc. Thermocouple T_{11} was used to measure the temperature of the chamber cooling water at various points along the chamber wall.

4.2.2 Combustion Chamber Temperatures

The mean temperature profiles for several transverse sections of the combustion chamber were determined by means of a Platinum-13% Rhodium/Platinum thermocouple which was inserted through the tappings shown in Figure 4.1.

A Metrohm potentiometric chart recorder was used to measure the emf of the thermocouple.

4.3 Exhaust Calorimeter

It was intended that the energy remaining in the exhaust gas should be determined from the gas temperature and composition. Unfortunately accurate measurement of the exhaust temperature was found to be impossible due to the alternating nature of the flow in the vicinity of the chamber port.

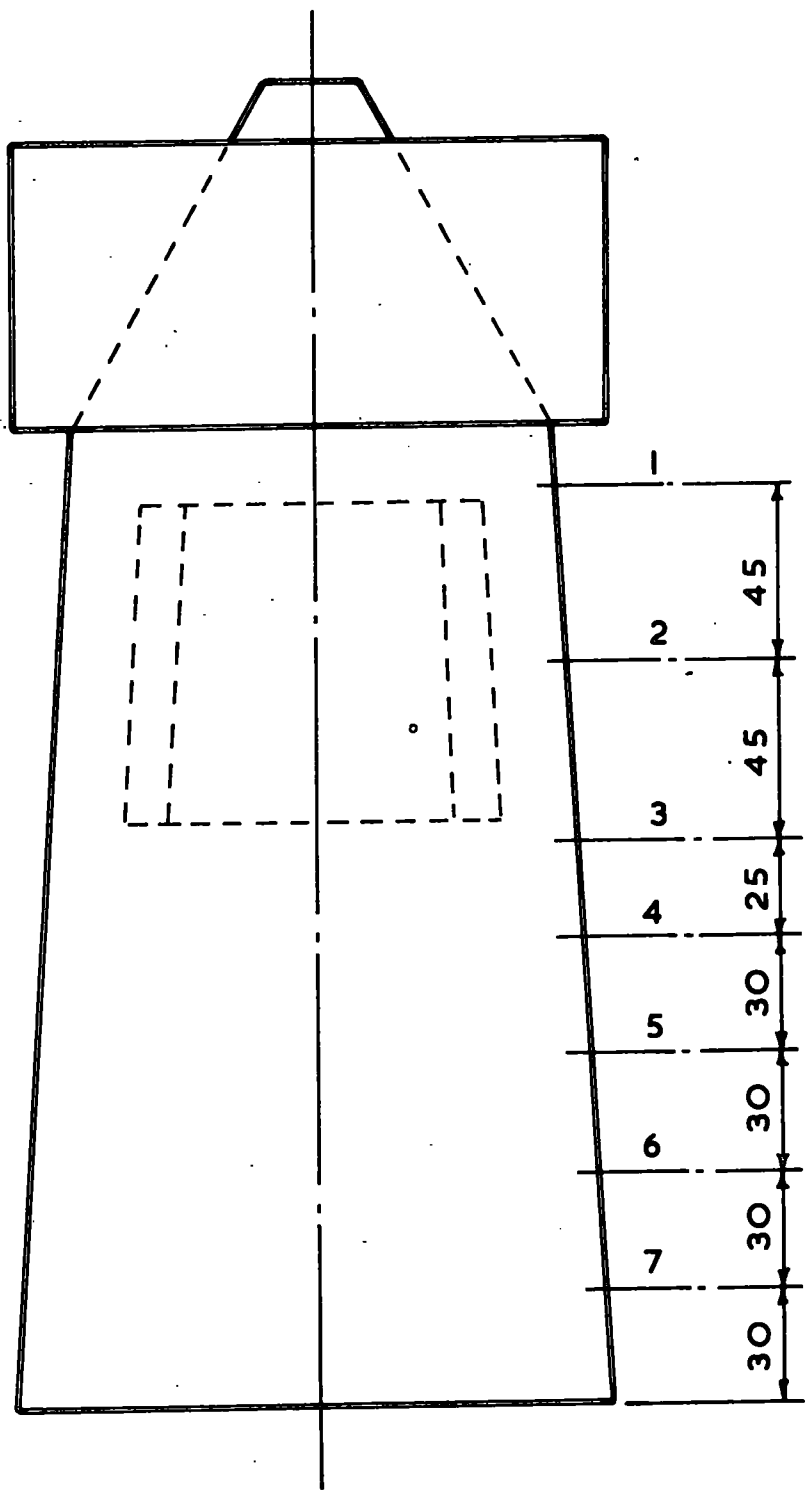

Dimensions in millimetres Scale: 1/2 Full Size

Figure 4·1 Tappings for Pressure Transducers, Ion Probes and Thermocouple.

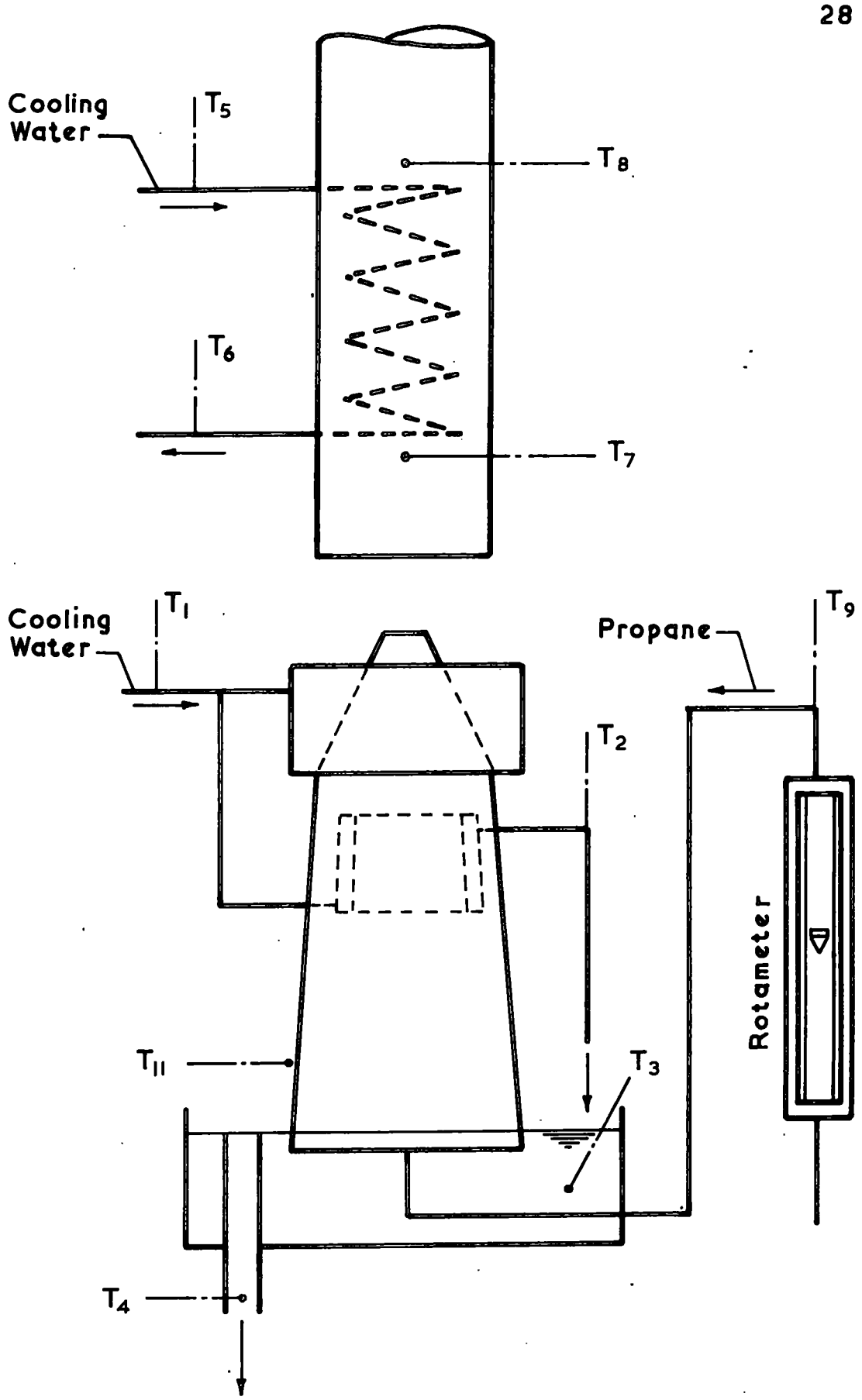

Figure 4·2 Temperature Points

A calorimeter section was therefore built into the flue pipe, as shown in Figure 4.2. The cooling coil for the calorimeter was made from 6m of 4.75 mm O.D. thin walled copper tubing wound into a close coiled helix, the helix being waisted so that the coil covered the full cross-section of the flue pipe.

The cooling water flow rate through the coil was determined by simply timing the discharge of a quantity of water.

Cooling water inlet and outlet temperatures and "exhaust"* temperatures before and after the calorimeter section were recorded using copper-constantan thermocouples and a Honeywell recorder (see section 4.2).

4.4 Measurement of Fuel Flow

In deciding on a method of measuring the propane flow the following points had to be taken into account.

1. The effect of the fluctuating chamber pressure on the operation of the meter.
2. The low flow rates; the fuel flow rate was expected to be in the range 0.01 to 0.03 m^3/min.
3. Facilities for calibrating the meter were not available.

A meter of the rotameter type was considered to be the most suitable. This type of meter was readily available in a size which adequately covered the expected flow range and

* Not the true exhaust temperature but the temperature of the mixture of exhaust gas and air in the flue pipe.

from data supplied by the manufacturers calibration curves could be constructed.

Regarding the latter, that is the construction of calibration curves for the meter, it was found impracticable to construct a calibration curve for each reading taken during a test and consequently the fuel supply system was designed to allow the pressure and temperature of the propane in the meter to be maintained constant. By maintaining constant conditions in the meter it was possible to use a single calibration curve to cover the full flow range.

Control of the gas pressure at the rotameter was achieved by fitting valves to the inlet and outlet of the rotameter. By means of these valves the pressure in the rotameter could be maintained constant at a value slightly higher than the maximum pressure required at the gas nozzle.

Maintaining a constant temperature at the rotameter did not present a problem since it was found that due to the extensive use of thin wall copper tubing between the gas bottle and the rotameter, the gas remained at ambient temperature over the full flow range.

To prevent damage to the rotameter occurring when the gas supply was turned on suddenly (the operation of the combustor required that the gas be turned on quickly for starting) a by-pass line was included in the system. The combustor could then be started with the rotameter isolated from the gas flow.

Gas pressure in the rotameter was measured with a mercury manometer and gas temperature was recorded on a multi-

point recorder, the temperature sensor being a copper-constantin thermocouple fitted in the outlet of the rotameter.

For reasons of safety the gas supply was controlled (on/off only) remotely by a pneumatic valve (5).

A diagram of the fuel supply system is shown in Figure 4.3.

4.5 Exhaust Sampling

The fact that the exhaust gas flow was intermittent created problems in exhaust sampling. The usual method of drawing a sample through a probe could not be employed since there was a risk of drawing in an unknown amount of air with the sample. It was found, however, that by directing the probe tip upstream the pressure of the exhaust on the probe tip was sufficient to cause a flow of exhaust gas through the probe and through the considerable length of flexible tubing connecting the probe with the gas analysis equipment. One problem still remained, however, and this was that the air entering the combustion chamber towards the end of the induction period might be blown back out and into the sampling probe. No way of avoiding this could be found and it has been accepted by the author that the gas analysis results might give an air/fuel ratio slightly higher than where combustion occurs.

Figure 4.4 shows the exhaust sampling probe in position over the chamber port and as can be seen from the figure the sample was taken from a point on the axis of the

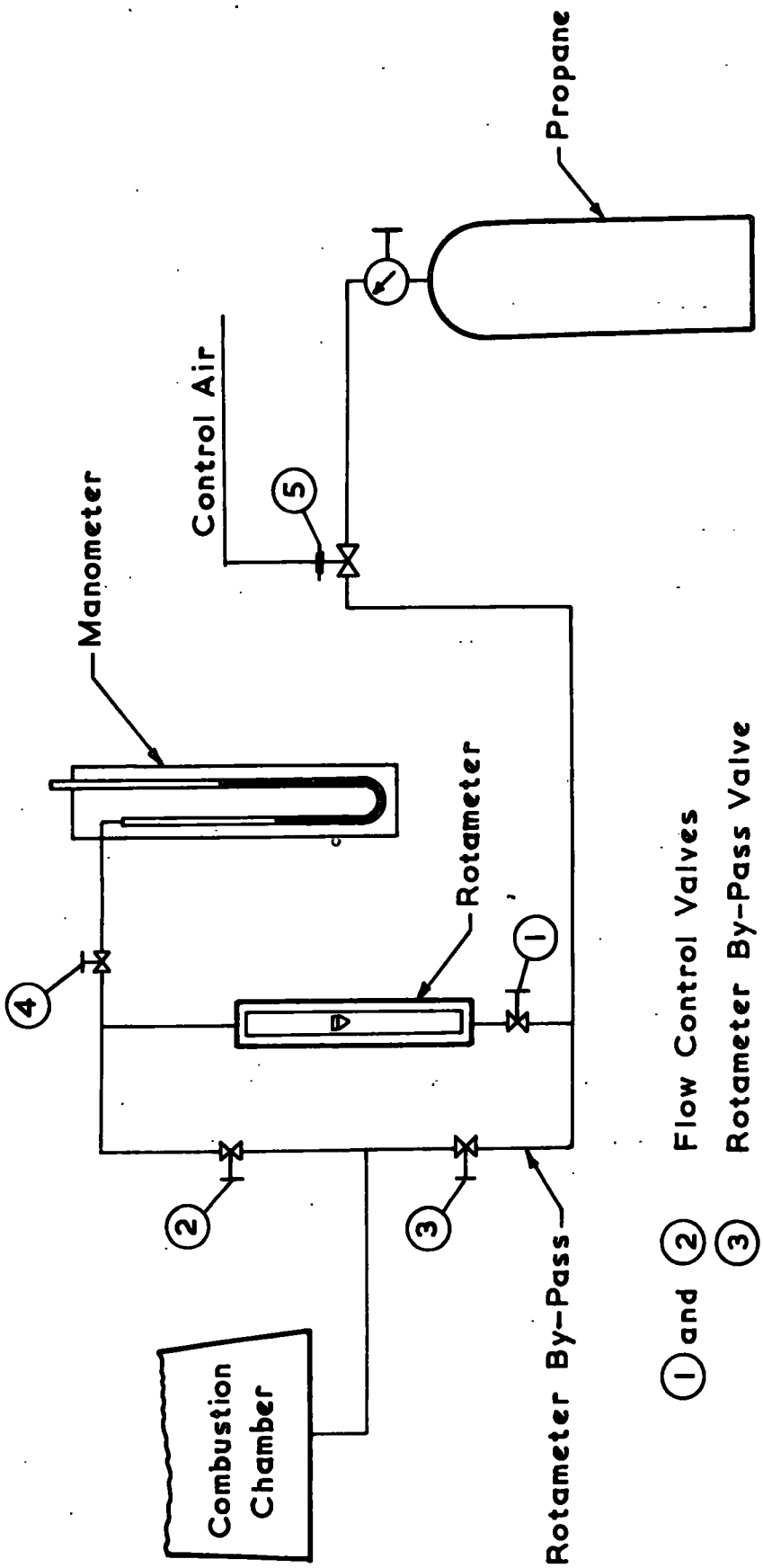

Figure 4·3 Propane supply and metering system.

Figure 4.4 Exhaust Sampling Probe

combustor just above the chamber port.

The author did not notice any significant change in the operation of the combustor due to the slight obstruction of the chamber port by the sampling probe.

4.5.1 Exhaust Gas Analysis

Initially gas analysis was carried out using Orsat apparatus. The Orsat was not equipped with a combustion vessel and therefore any hydrocarbons present in the exhaust could not be detected. However, since the results showed that oxygen was present it was considered unlikely that there would also be hydrocarbons.

Towards the end of the tests a gas chromatograph became available. This chromatograph required a number of modifications before it could be used for exhaust gas analysis and a considerable amount of time was spent on its development. For a complete analysis of the exhaust gas two columns were used in parallel, one containing molecular sieve 5A and the other containing silica gel. The chromatograph had only one detector which was of the thermal conductivity type and to use two columns with one detector involved joining the outlets of the columns together before connecting them to the detector; all connections were made with capillary tubing (metal). Using two columns in parallel proved difficult and a great deal of cut and try was required before correct operation was achieved and even then the analysis time was long (about 25 mins) and the peaks tailed badly.

To improve the chromatograph a sampling valve was fitted

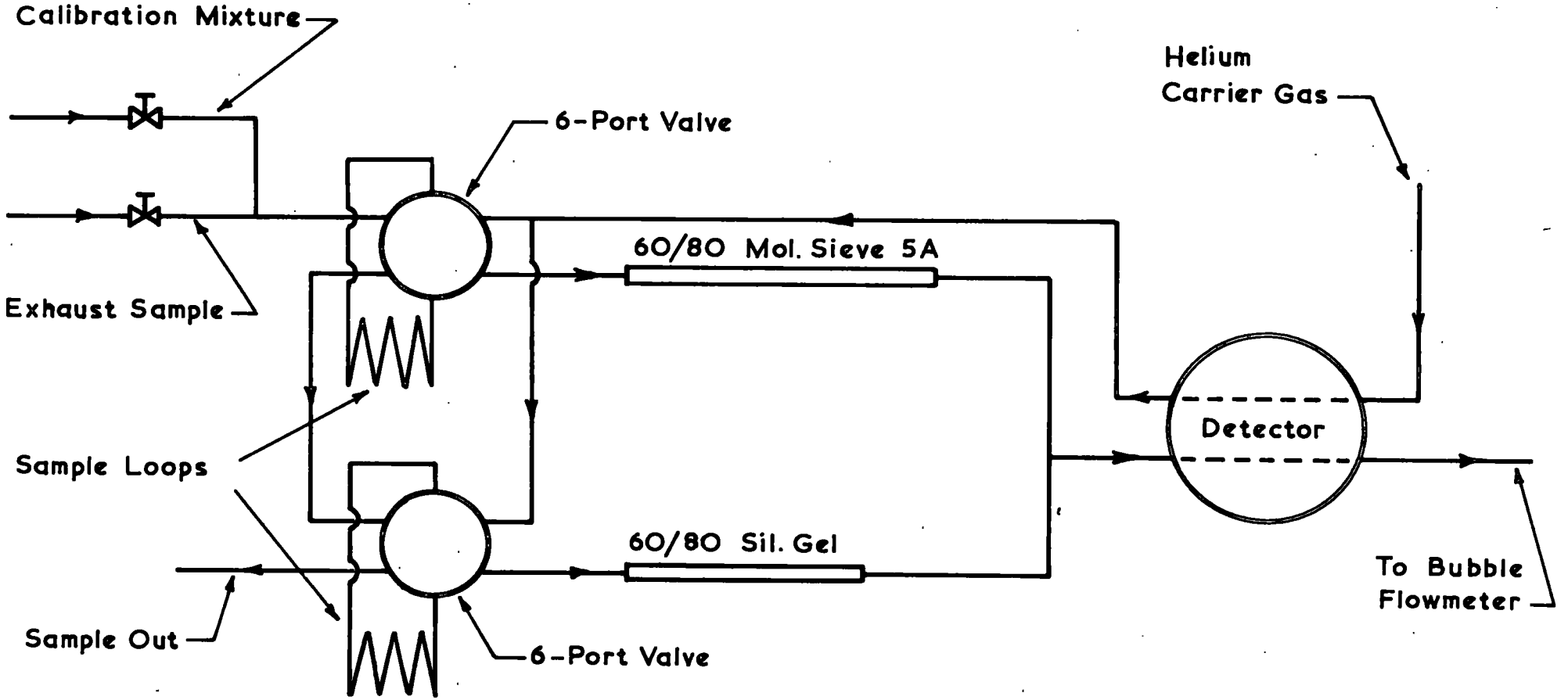

Figure 4·5 Arrangement of columns and sampling valves for Shandon UK3 Gas Chromatograph.

to each column. This enabled the sample size to be set to suit the particular column, thereby giving a combination of short analysis time and maximum peak height on the recorder. Details of the chromatograph are given in Figure 4.5.

4.6 Ionization Flame Detection

Details of an ion probe developed for the purpose of determining flame speed are given in Figure 4.6. The method of determining flame speed consisted of measuring the time interval between corresponding signals received from two probes situated a small distance apart on the line of propagation of the flame. The probe positions used in the flame speed tests are shown in Figure 4.1.

Owing to the high impedance of the electrode gap under ionizing conditions, the current flowing in the detector circuit was extremely small (less than 1uA), however by connecting an oscilloscope in the probe circuit as shown in Figure 4.6 with the oscilloscope set on d.c., voltage signals of up to 25V were obtained. With the oscilloscope set on a.c. the signals were much smaller.

Condensate picked up by the probes from the wall of the combustor when they were inserted presented a problem since it effectively short circuited the ionization gap, thereby rendering the probes inoperative. This was overcome by ensuring that the probes were inserted far enough into the chamber for the moisture to be driven off before they were retracted to the required position near to the wall.

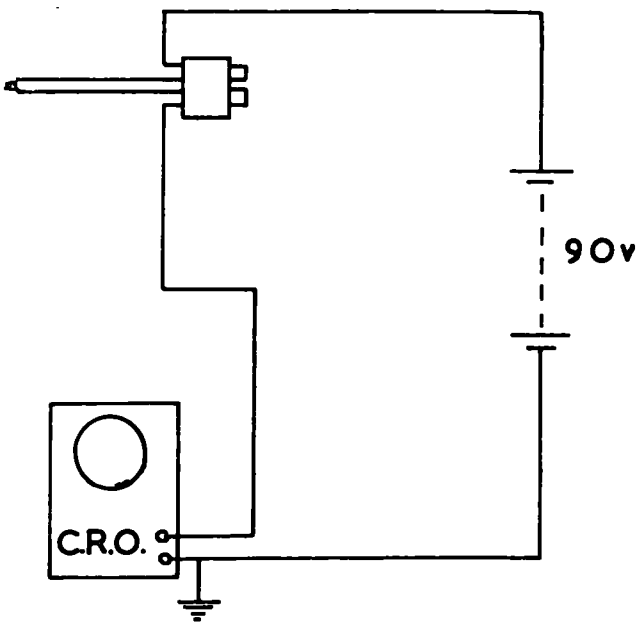

CIRCUIT DIAGRAM

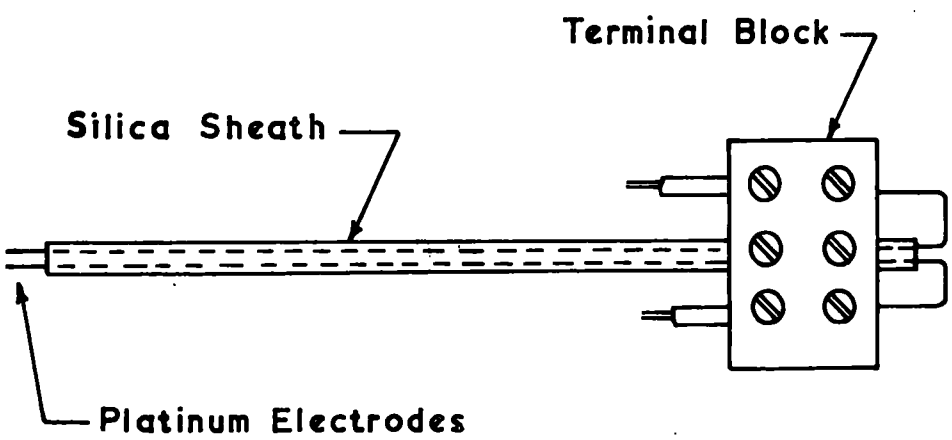

Figure 4·6 Ionizatation Flame-Detector (Ion Probe).

4.7 Radiation Measurements

The fluctuations in the level of radiation from the gases in the combustion zone (this may be taken to be the space between the internal nozzle and the base plate) were recorded using a Silicon phototransistor - Mullard type BXP25 and Germanium phototransistor - Mullard type OCP71. Diagrams of the Relative Spectral Response for the transistors are given in the appendix. From these diagrams it can be seen that both types of phototransistor are sensitive mainly to radiation in the near infrared region.

Tests were also carried out using the OCP71 phototransistor with an infrared absorbing filter fitted to restrict the radiation reaching the phototransistor to the visible region. This was done in order to distinguish between the radiation from the flame and that from the hot gases.

To compare the fluctuations in radiation level with the fluctuations in pressure during a cycle the output from a phototransistor was displayed on one channel of a double beam oscilloscope, the other channel of the oscilloscope being used for the output from a pressure transducer.

Results were obtained from the OCP71 phototransistor mounted in the flue pipe immediately above the chamber port and from both the BXP25 and OCP71 phototransistors mounted at the end of a small tube fitted in a window in the combustor wall. This latter mounting was also used for the combination of OCP71 phototransistor and infrared absorbing filter. The position of the window can be seen in Figure 4.7.

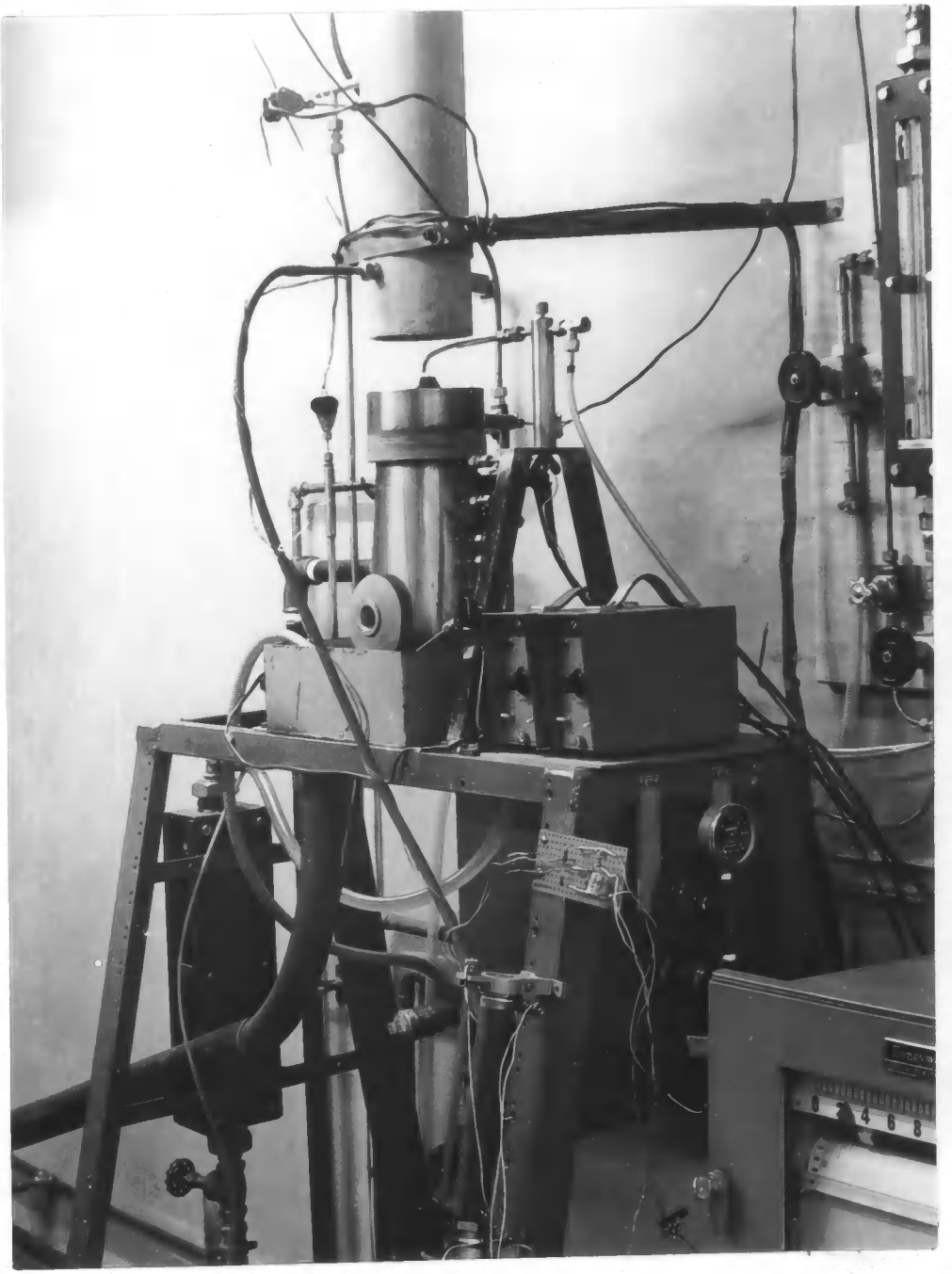

Figure 4.7 View of rig showing window in combustor wall.

4.8 Frequency/Fuel Flow Tests

Tests were carried out to determine the relationship between the frequency of the combustion cycles and the rate of fuel flow. Two methods were used in determining combustion frequency; these were (a) measuring the frequency of the signal from a pressure transducer by means of a timer counter and (b) counting the peaks on a U.V. recorder trace of chamber pressure.

Frequency by Timer Counter

At first this method proved unreliable at low rates of fuel flow due to the signal from the pressure transducer/charge amplifier being below the minimum required by the counter. This was corrected by the use of an additional amplifier but care was required in using the second amplifier since it was found that too high a gain on this amplifier could cause the counter to go erratic, probably owing to a combination of noise and irregularities in the pressure wave-form triggering the counter.

An Advance Timer-Counter type TC1A and a Hewlett Packard Electronic Counter type 3734 were used in these tests.

Frequency from U.V. Recorder Trace

The disadvantage of this method was that to attain the same order of accuracy as the electronic counters some 250 peaks had to be counted for each result with the attendant risk of miscounting.

However, the chances of a large error with this method were much lower than with the electronic counters and the method, therefore, provided a useful check.

4.9 Miscellaneous Experiments

4.9.1 Effect of Cooling Water Temperature on Combustor Operation

To test the operation of the combustor at high cooling water temperatures the cooling system described in 3.5.1 and used in previous tests was modified. The modifications consisted of installing a tank to collect the waste water from the chamber so that this water could be recirculated. A supply of cold make up water was also provided to enable the cooling water temperature to be stabilised at any required value.

Preliminary tests under recirculating conditions without make up water showed that the chamber stopped operating at about 160^{o}F. Further tests were therefore carried out to determine the maximum temperature at which the chamber could be considered to be reliable.

4.9.2 Observations Using a Stroboscope

A simple stroboscope was made by fitting a slotted disc to the shaft of a small d.c. motor; the speed of the motor was controlled by a rheostat. Using the stroboscope the combustion was observed through the window in the chamber wall (Figure 4.7) and through the chamber port.

A special base shown in Figure 4.8 was manufactured for the observations using the stroboscope, but unfortunately the pyrex glass used for the windows was unable to withstand the severe conditions.

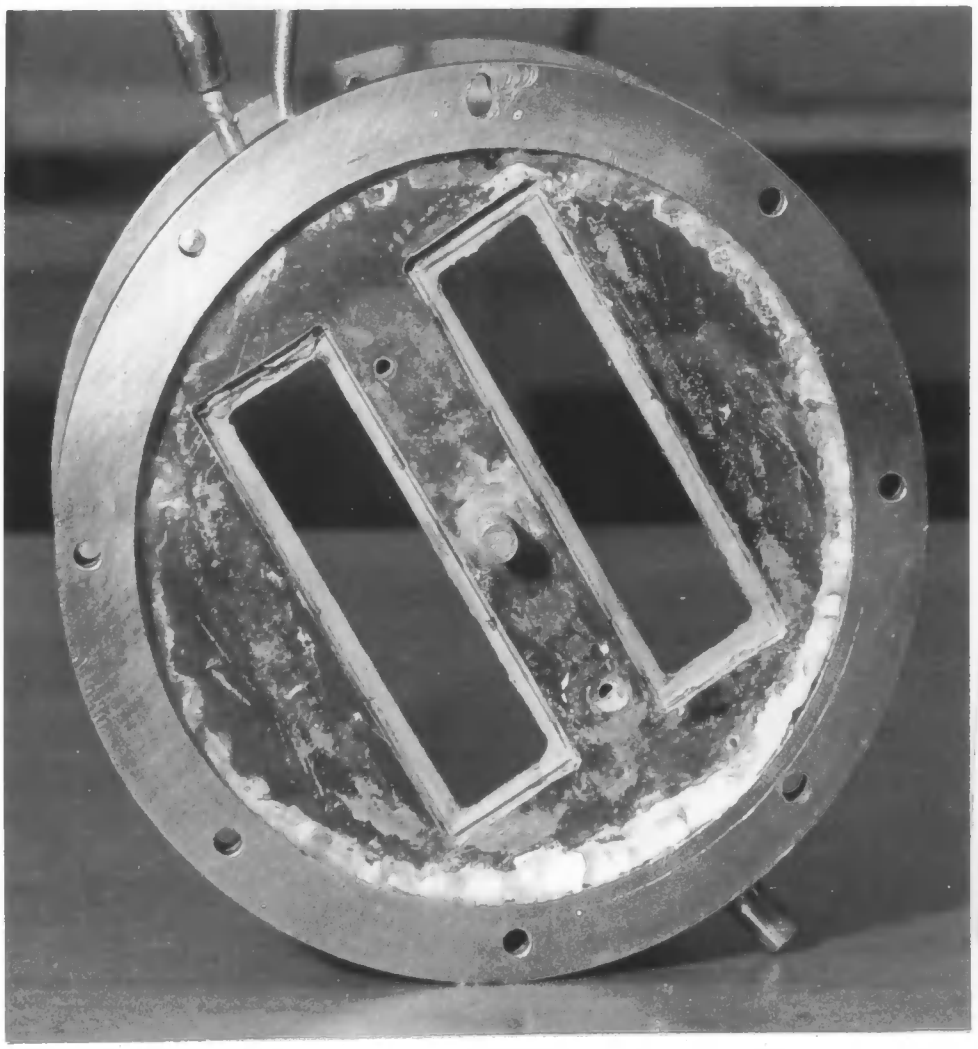

Figure 4.8 Base with windows

4.9.3 Combustor Noise

An analysis of the sound emitted by the combustor was made using a Bruel and Kjaer frequency analyser type 2107. Sound spectrograms were obtained for three rates of fuel flow and from these spectrograms overall noise levels were determined. For the above measurements a 25.4 mm condenser microphone was used; the microphone was placed 1 m from and level with the chamber port. Spectrograms of background noise were also obtained.

5. RESULTS

5.1 Combustion Chamber Pressure

Figure 5.1

This diagram, which was taken from an oscillogram shows a typical (smoothed) pressure cycle. The atmospheric line was obtained by using a strain gauge pressure transducer with a double beam oscilloscope, the technique being to set both beams of the oscilloscope to coincide before starting the combustor. The combustor was then started and the trace was photographed. Before using this method the output from the transducer was checked to establish that drift was not significant.

Due to the possibility that wave action made an important contribution to the 'breathing' of the combustor it could not be assumed that exhaust and induction periods started and ended when the chamber pressure was atmospheric. It was, therefore, necessary to determine the start and finish of the exhaust period (and hence the induction period). This was done by detecting the flow of gas from the chamber and comparing this with a pressure diagram. The method of detecting the gas flow consisted of placing the exhaust sampling probe in the exhaust stream and recording the variation of stagnation pressure in the probe by means of a pressure transducer fitted to the probe outlet.

The first attempt using the above method was made with a diaphram transducer from a Farnboro indicator but although the 'Farnboro' transducer detected the exhaust flow it did not

respond to small pressure differences so that errors in timing the exhaust flow occurred. The 'Farnboro' transducer was, therefore, replaced by a strain gauge transducer which was more sensitive. Figures 5.2 and 5.3 show the results obtained with the 'Farnboro' transducer and the strain gauge transducer respectively.

Figure 5.4

This Figure relates maximum and minimum values of chamber pressure to the rate of fuel flow for flow rates in the range 0.015 to 0.025 m^3/min. Each value of pressure shown on the diagram is an average value taken over 20 cycles.

5.2 Temperature Measurements

Figure 5.5 Mean Temperature Profiles

The above diagram shows mean temperature profiles for chamber sections 1 to 7 (Figure 4.1) of the chamber.

It was found when obtaining the data for chamber section 3 that the reading at a point 14 mm from the chamber centre line could take on one of two widely different values, one value being 3.05 mv and the other 5.1 mv. At first this rather odd effect did not appear to have any particular pattern of occurrence, but since it cast doubt on the validity of the readings obtained for other points it was important to determine its cause.

Further tests showed that the 5.1 mv reading always

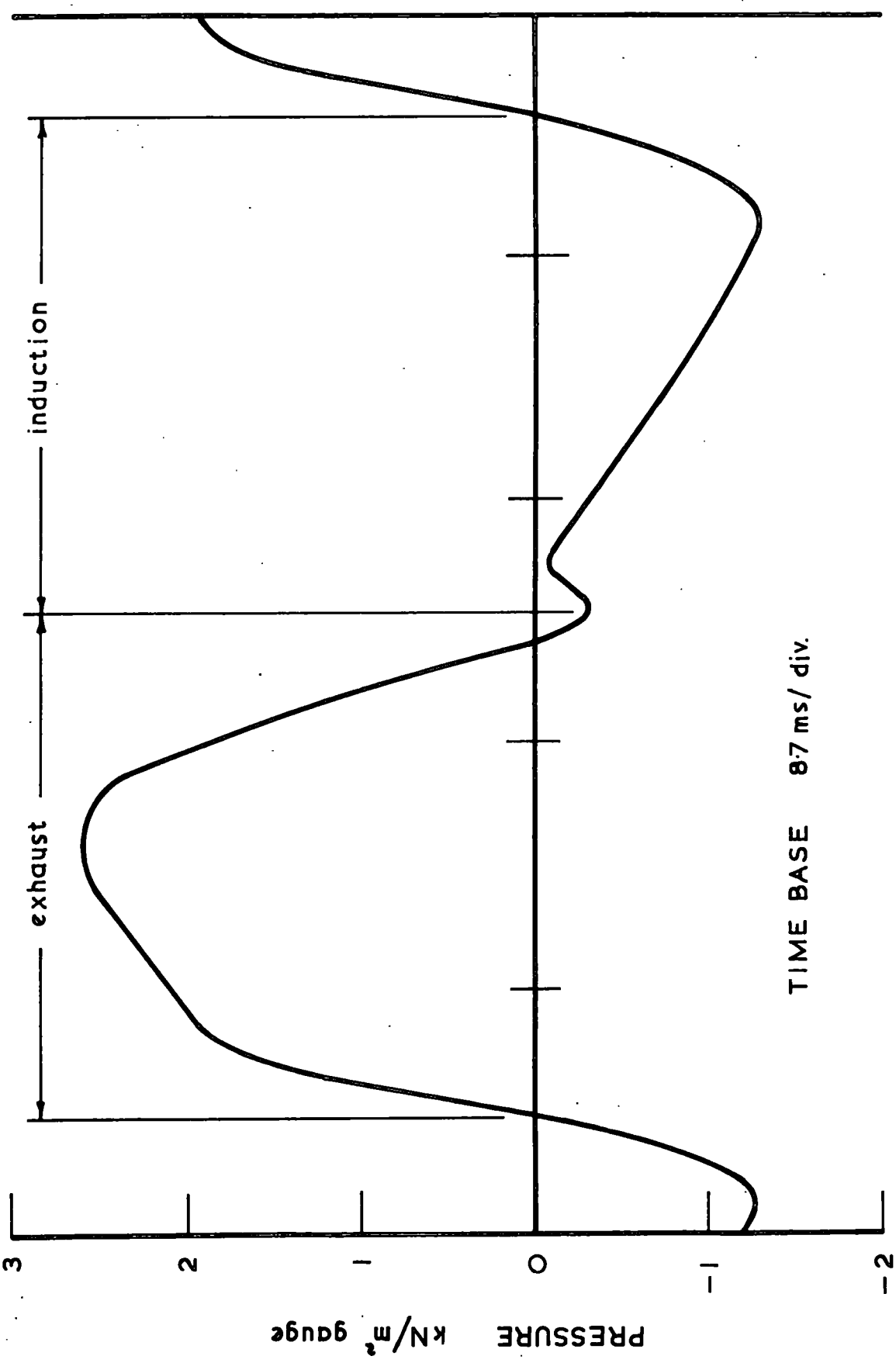

Figure 5·1 : Pressure—Time Diagram.

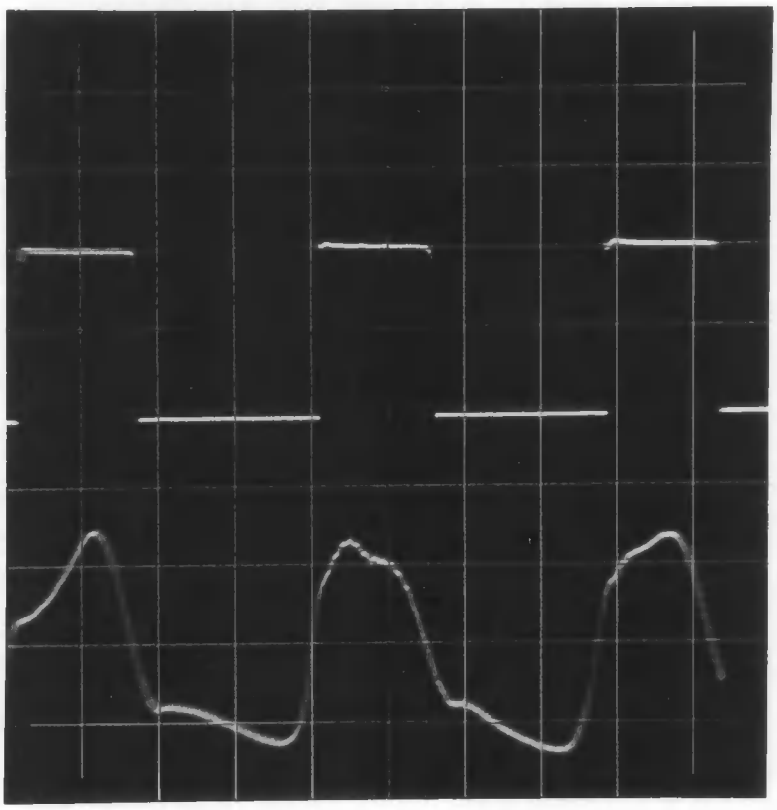

Figure 5.2 Duration of exhaust flow (upper trace) recorded with 'Farnboro' type pressure transducer.

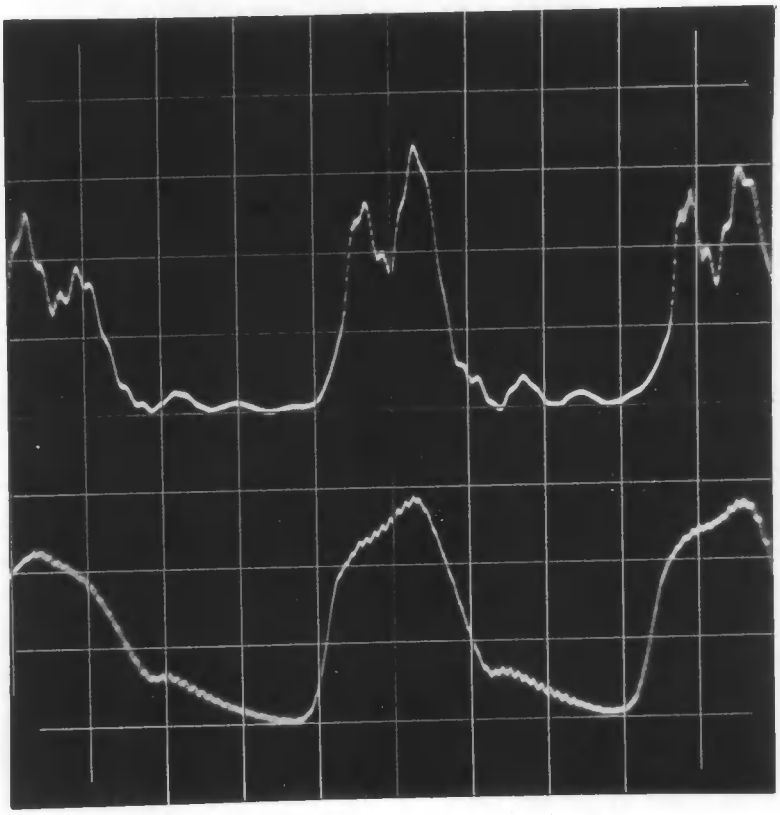

Figure 5.3 Duration of exhaust flow (upper trace) recorded with strain gauge pressure transducer.

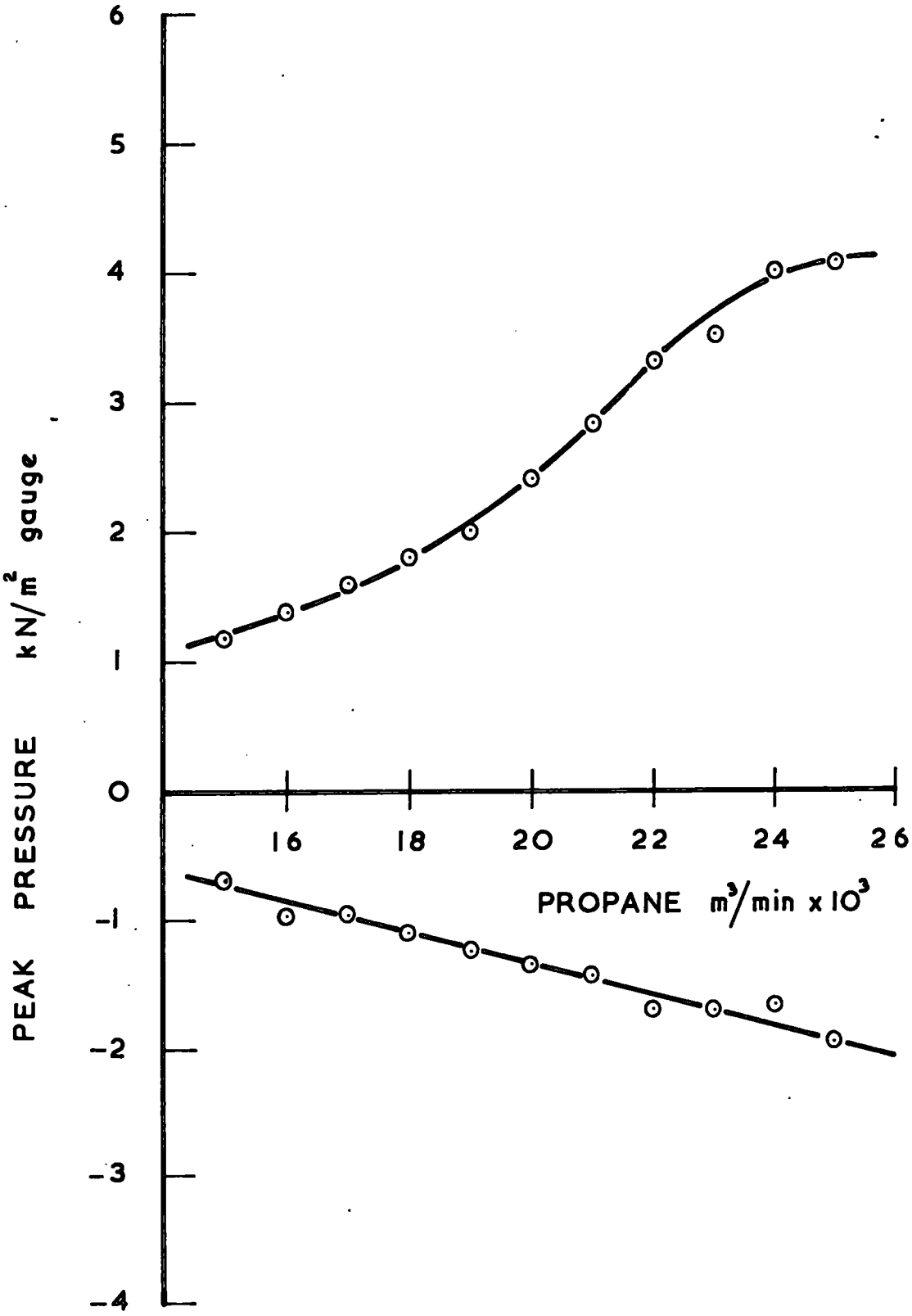

Figure 5·4 Variation of Peak Pressure with Fuel Flow.

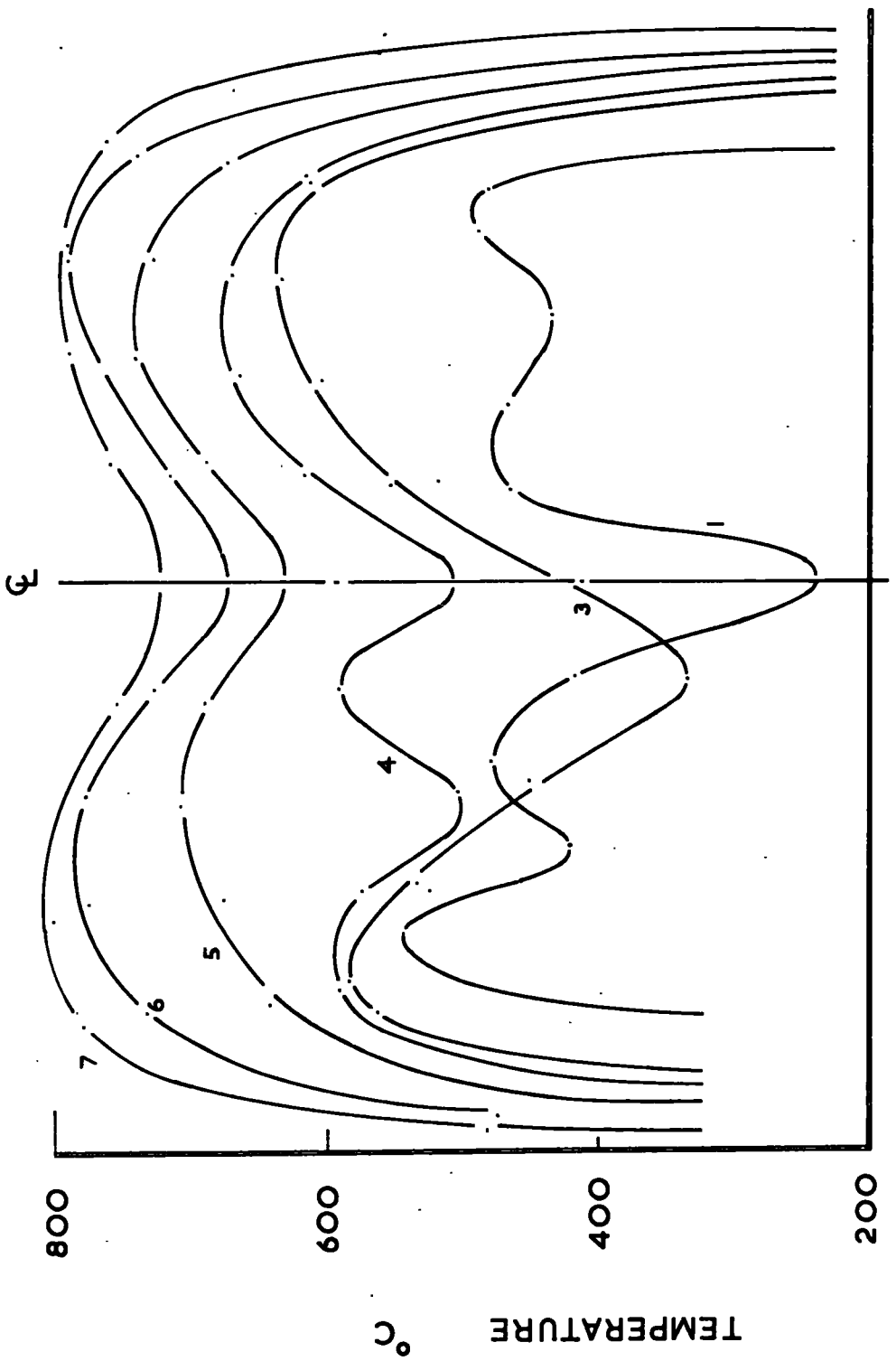

Figure 5·5 Mean Temperature Profiles: Sections 1 to 7.

occurred when the probe was moved from the wall inwards to the required position and that the 3.05 mv reading occurred when the probe was moved from the centre line outwards to the required position. The movement of the probe was then observed through the chamber port with the aid of a stainless steel mirror which revealed that the thermocouple bead remained incandescent when moved inwards to the position 14 mm from the chamber centre line. That is, after passing through a hot zone the bead did not cool down to the normal temperature of the point measured. One possible explanation is that the bead acted as a flame holder and enabled the reaction in its vicinity to continue, thereby affecting the mean temperature in its vicinity. When the bead was moved from the cold central region of the chamber the above effect did not occur. It has, therefore, been assumed that 3.05 mv was the undisturbed value.

5.2.1 Combustion Chamber Isotherms (for mean temperatures)

These are shown in Figure 5.6 and were obtained from the mean temperature profiles of Figure 5.5. In order to draw the isotherms a certain amount of interpolation was necessary and for accuracy this interpolation was carried out by drawing mean temperature profiles for vertical sections.

5.3 Exhaust Calorimeter

The calorimeter described in section 4.3 failed to give useful results. This was mainly due to the fact that the hot exhaust gas did not have sufficient time to mix with the

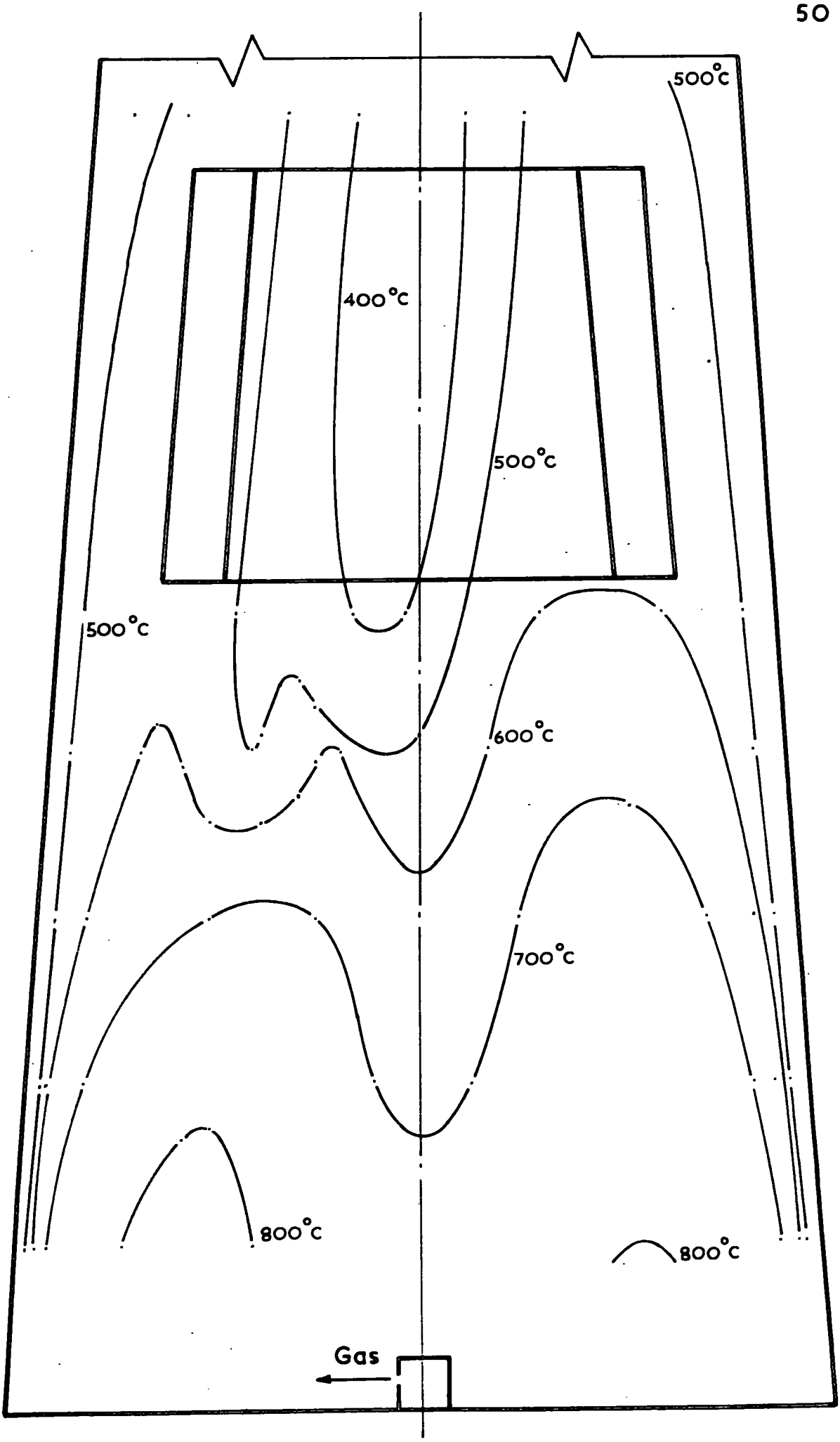

Figure 5·6 Isotherms for Mean Temperatures.

air that was also drawn into the flue pipe by the extractor fan before reaching the cooling coils. The design of the calorimeter section was limited by the head room in the test cell (in which the rig was installed) so that modifications to provide a greater mixing length were not possible.

5.4 Exhaust Gas Analysis

The chromatograph as described in section 4.5.1 could not be used for quantitative work owing to unexpected defects in the sampling valves. These valves were found to have serious cross port leakage which could not be corrected. Another type of sampling valve was tried on single column operation and found satisfactory. Unfortunately this type of valve was not suitable for dual column operation.

After consideration it was decided that the problem of exhaust gas analysis could best be solved by using a single column chromatograph for Oxygen, Nitrogen and Carbon Monoxide determination and an Orsat for Carbon Dioxide. This method was expected to give a complete analysis without the need to obtain one component by difference. Preliminary results obtained with the above method showed a discrepancy of approximately 3% and it was clear that some constituent of the gas mixture was not being detected. The undetected component was believed to be Hydrogen, since (i) Carbon Monoxide was present, and (ii) Hydrogen would not show on the chromatogram owing to its thermal conductivity being similar to that of Helium which was used as carrier gas.

To check for the presence of Hydrogen a sample of exhaust

gas was analysed on a Pye Series 104 chromatograph using Argon as carrier gas; the analysis shows 1 to 2% Hydrogen in the sample.

The method of gas analysis finally adopted involved using the two chromatographs and an Orsat (to check CO_2). Particulars of the chromatographs are given in the Appendix and typical chromatograms are shown in Figures 5.7 and 5.8

5.5 Air/Fuel Ratio

Owing to the fact that not all of the air entering the combustor went into the combustion chamber (some air was drawn directly into the exhaust pipe by the ejector action) it was impossible to determine the air/fuel ratio by direct measurement of the air and fuel flows. Air/fuel ratio was therefore calculated from the exhaust gas analysis. Figure 5.9 shows the variation of air/fuel ratio with fuel flow rate, determined by Orsat analysis of the exhaust gas and by chromatograph analysis of the exhaust gas; of these two methods of gas analysis the latter is considered to be the most accurate.

5.5.1 Combustion Efficiency

Variation of combustion efficiency with fuel flow rate is shown in Figure 5.10.

The combustion efficiency, which is defined as 'energy released per unit mass of fuel/H.C.V. of fuel' was calculated from the exhaust gas analysis.

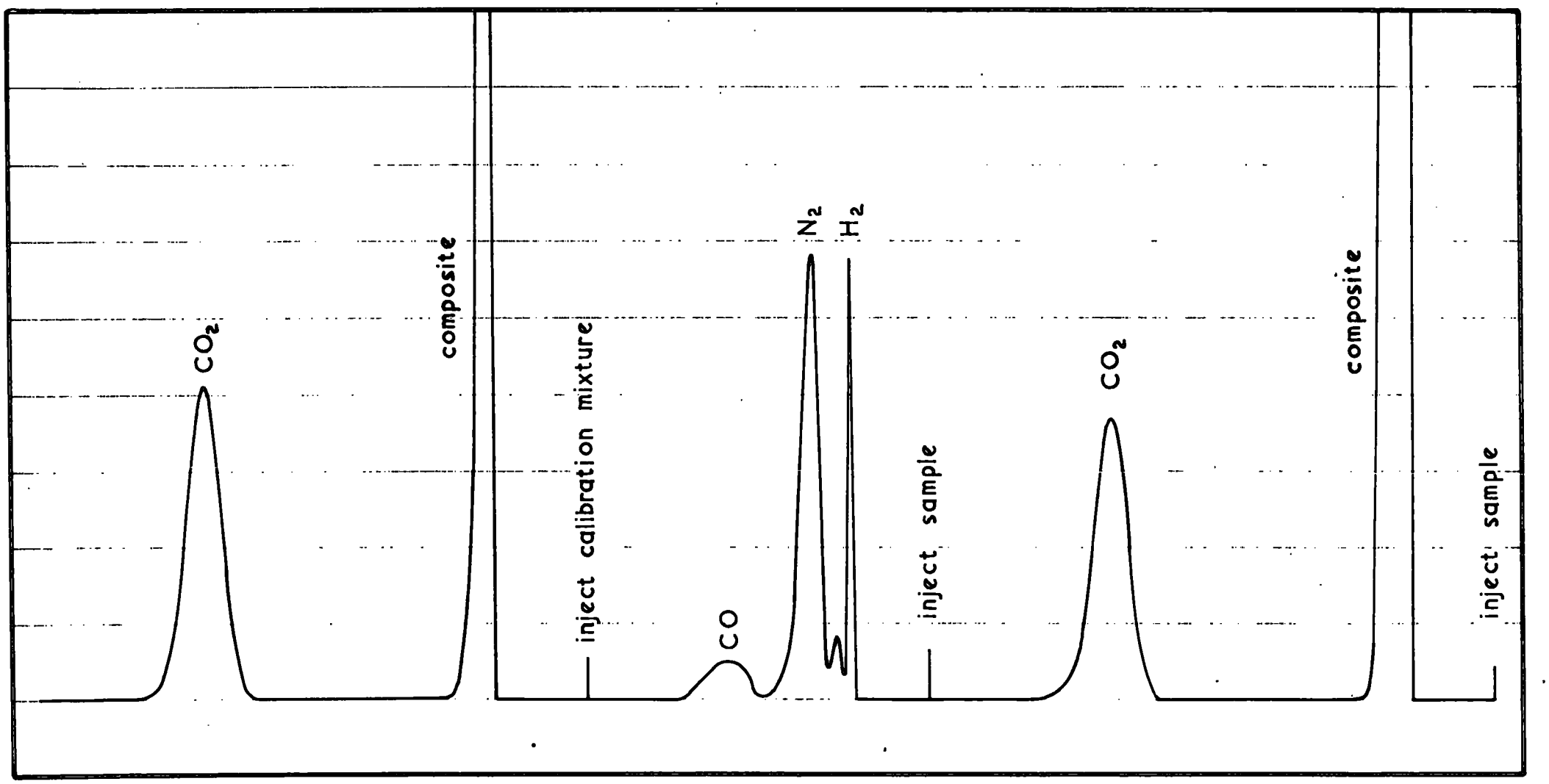

Figure 5-7 Chromatogram from Pye Series 104 Gas Chromatograph.

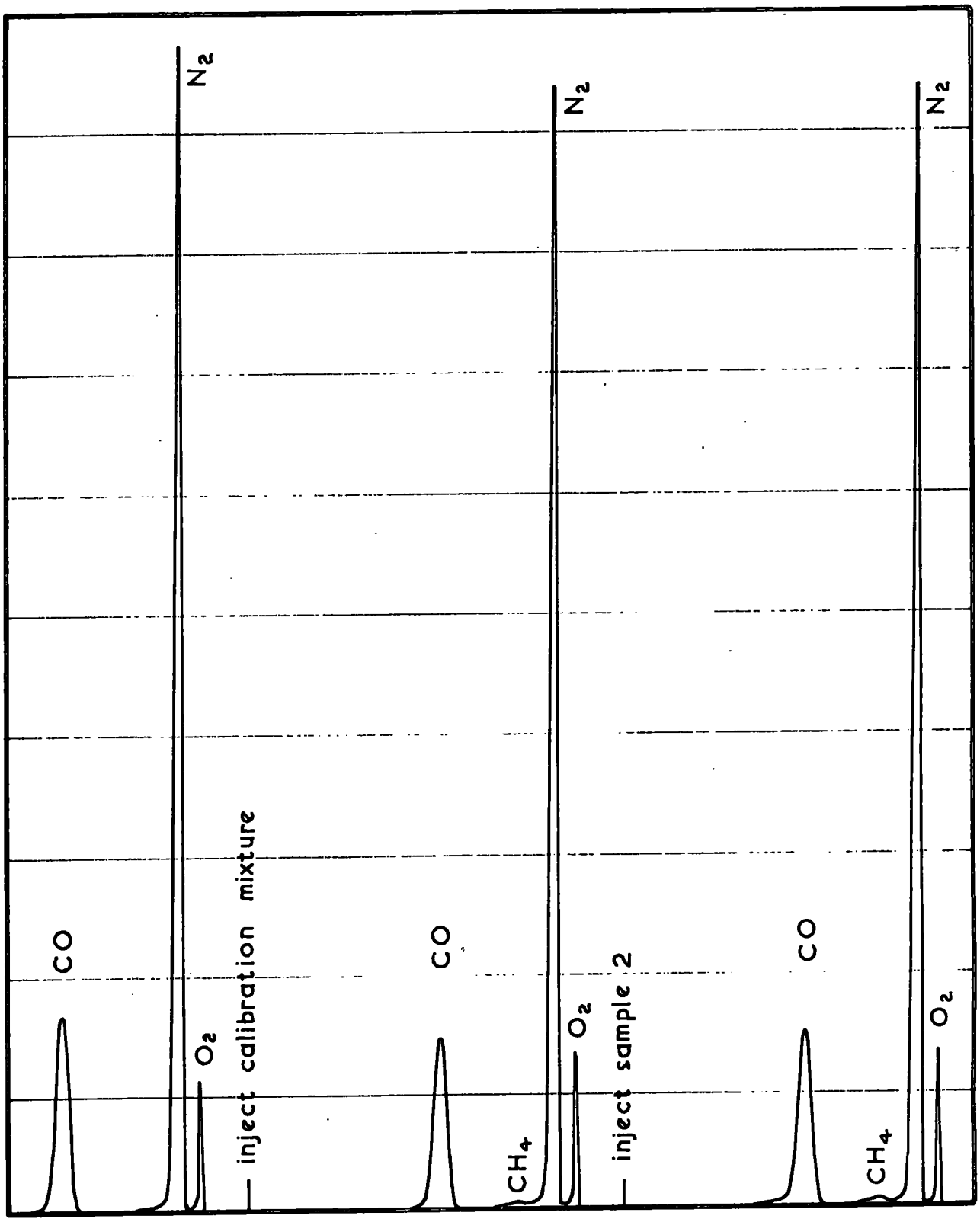

Figure 5·8 Chromatogram from Shandon UK3 Gas Chromatograph.

5.5.2 Combustion Intensity

The rate of energy release of the combustor was determined from the fuel flow rate and corresponding combustion efficiency. On this basis the combustion intensity (output per unit volume) was calculated and the maximum value for reliable combustor operation* found to be 8.25 MW/m^3; this value represents an output of 33 kW.

5.6 Ion Probe Results

Figures 5.11, 5.12 and 5.13

Figure 5.11 shows the outputs from two probes, the upper trace being from a probe in position 3 (Figure 4.1) and the lower trace from a probe in position 7. The probes projected 12.5 mm through the wall of the combustor. In Figures 5.12 and 5.13 the upper traces are from probes in positions 2 and 1 respectively whilst the lower traces are from a probe in position 7.

The above results were obtained for a fuel flow of 0.021 m^3/min. using a negative earth electrode.

* Occasionally the combustor would operate at a fuel flow of 0.025 m^3/min. but operation at this flow rate rarely lasted more than a few minutes before the combustor cut out.

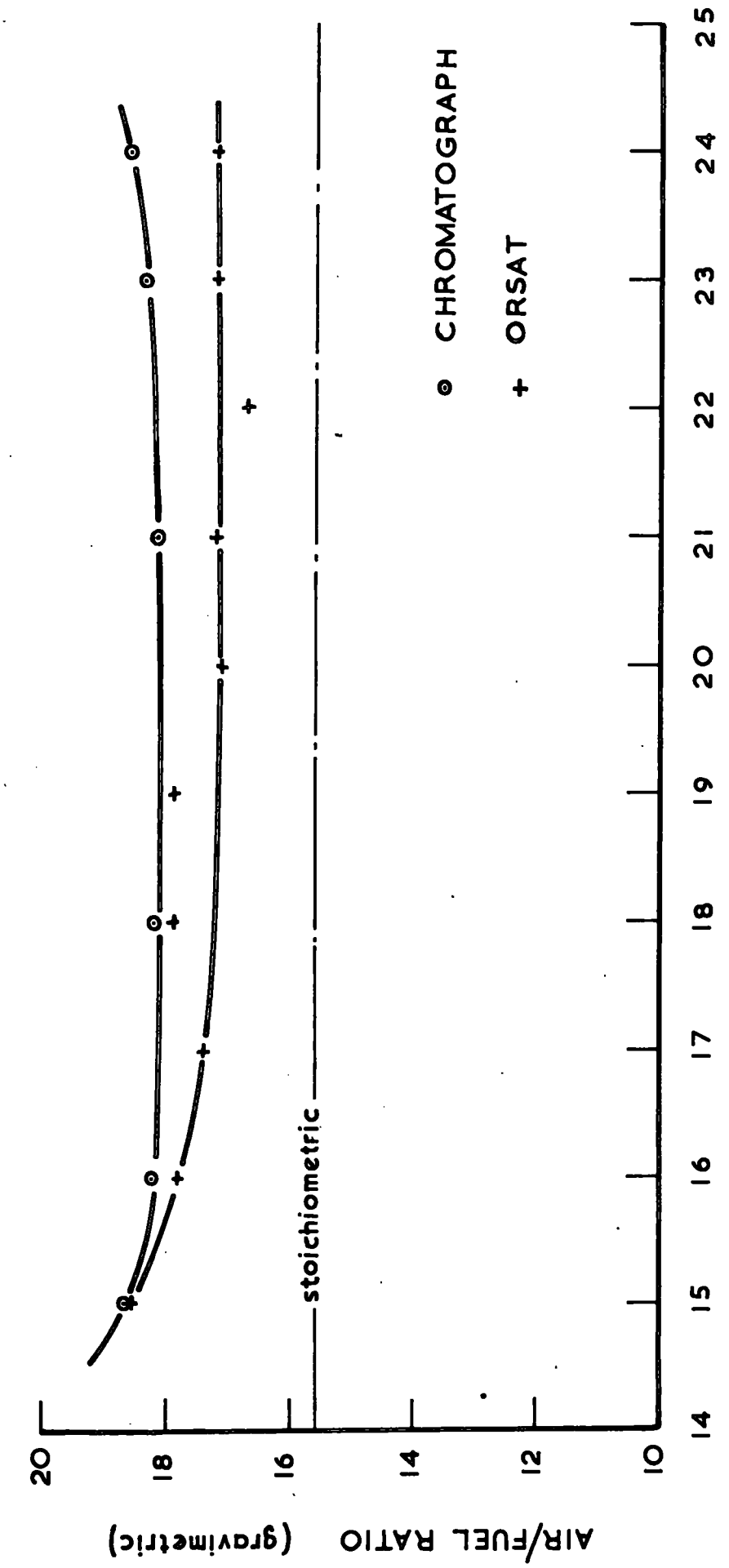

Figure 5·9 Air/Fuel Ratio

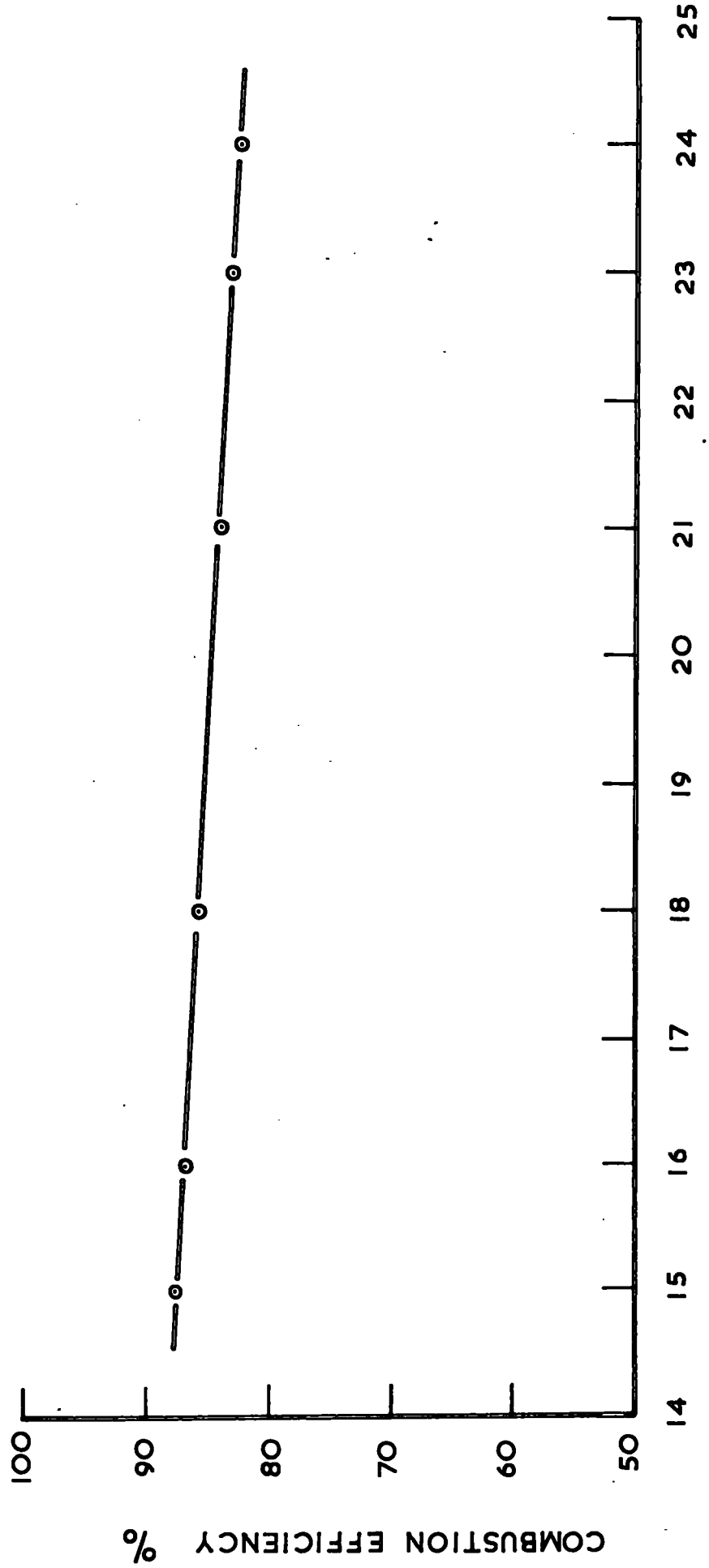

Figure 5·10 Combustion Efficiency

Figure 5.11 Signals from ion probes in positions 7 (upper trace) and 3 (lower trace). Time base 8.7 ms/div.

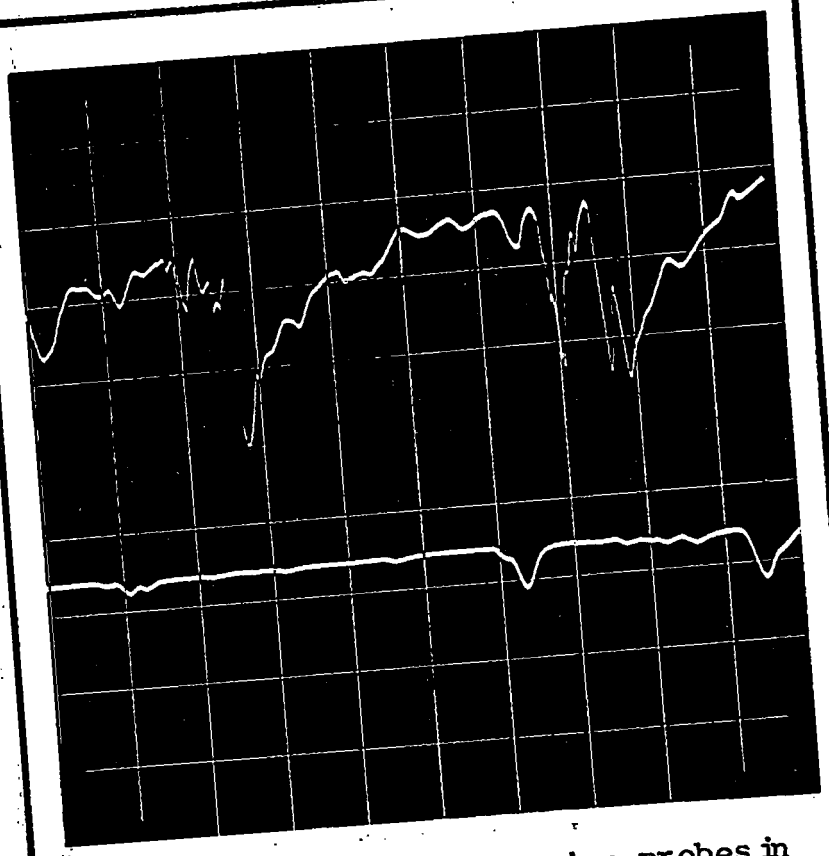

Figure 5.12 Signals from ion probes in positions 7 (upper trace) and 2 (lower trace). Time base 8.7 ms/div.

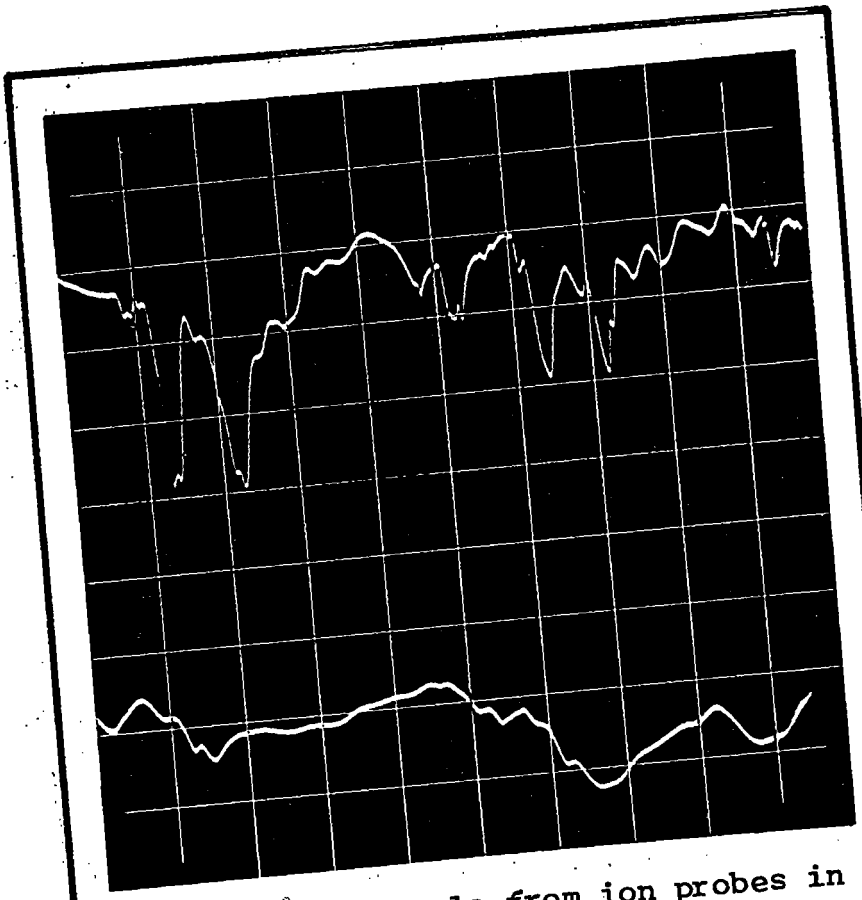

Figure 5.13 Signals from ion probes in positions 7 (upper trace) and 1 (lower trace). Time base 8.7 ms/div.

5.7 Radiation/Time Records

Figure 5.14

This Figure shows the output (top trace) obtained from the OCP71 phototransistor mounted in the window in the combustor wall as described in section 4.7.

The base line (lower trace) was produced by cutting off all light to the phototransistor.

Figure 5.15

Upper trace:- output from piezo-electric pressure transducer mounted in position 6.

Lower trace:- output from the OCP71 phototransistor mounted in window.

Figure 5.16

Upper trace:- piezo-electric pressure transducer in position 6.

Lower trace:- OCP71 phototransistor mounted above chamber 'looking' through chamber port.

Results from Phototransistor type BXP25

This type of phototransistor did not respond to the radiation from the flame or hot gases. As a check the phototransistor was exposed to the light from a stroboflash and the output was displayed on an oscilloscope. The check established that the device was functioning correctly.

Results from Phototransistor type OCP71 when used with an Infrared Absorbing Filter

With the filter fitted the radiation reaching the

phototransistor was in the visible range only. The phototransistor did not show any response to this radiation.

5.8 Frequency/Fuel Flow Results

Figure 5.17

The frequency/fuel flow characteristic for the combustor is shown in Figure 5.17. This diagram was plotted from the data obtained with the Hewlett Packard counter, which proved to be the more suitable of the two counters mentioned in section 4.8. The reason for this was the fact that the Hewlett Packard counter operated on a negative pulse, whereas the T.C.I.A. counter operated on a positive pulse and the negative part of the pressure wave form was much smoother and more regular than the positive part. Negative pulses were, therefore, more reliable as trigger pulses.

The limits of the standard deviation shown on the diaram refer to the standard deviation of twenty separate sample counts taken for each frequency. Variation of periodic time from cycle to cycle was considerably greater than the above standard deviation at the corresponding fuel flow. This can be seen by comparing the periodic time of the 'typical' cycle shown in Figure 5.1 with the value based on a frequency of 24.7 H_z (corresponding to a fuel flow of 0.021 m^3/min.) taken from Figure 5.17.

Helmholtz Frequency of the Combustor

The Helmholtz frequency of the combustor at ambient temperature was determined experimentally using a vibrator driven by a Bruel and Kjaer Sine Random Generator type 1024.

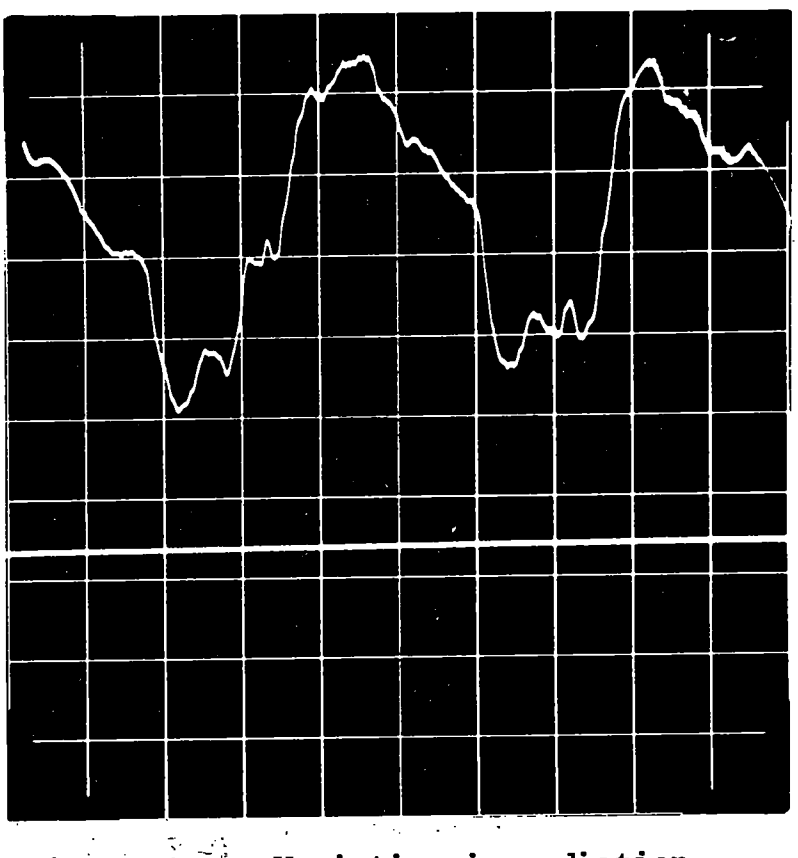

Figure 5.14 Variation in radiation intensity recorded with phototransistor OC71 mounted in window.

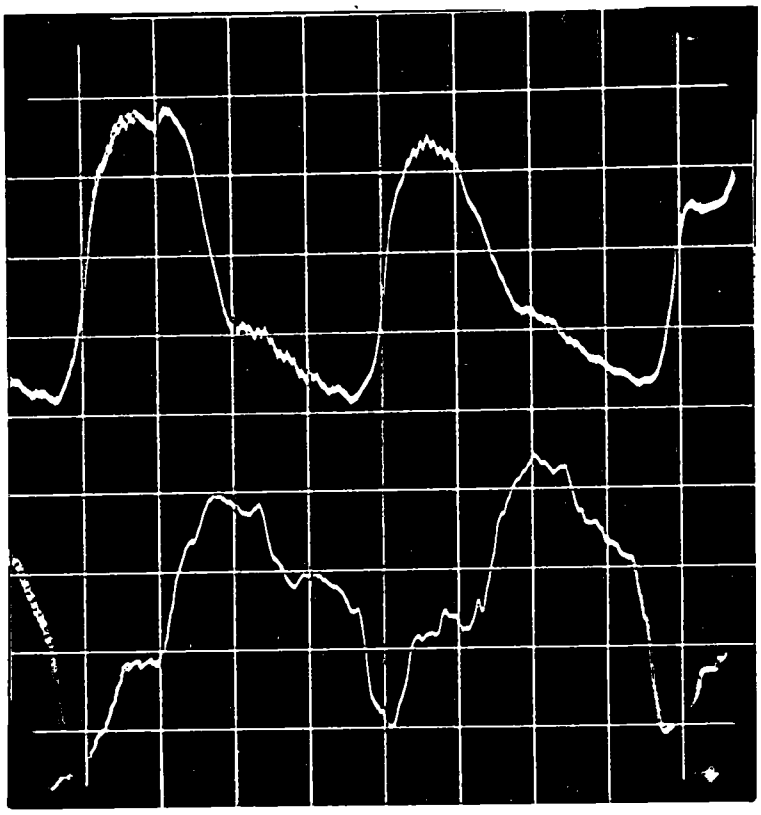

Figure 5.15 Upper trace: combustion chamber pressure. Lower trace: radiation intensity (0C71 mounted in window)

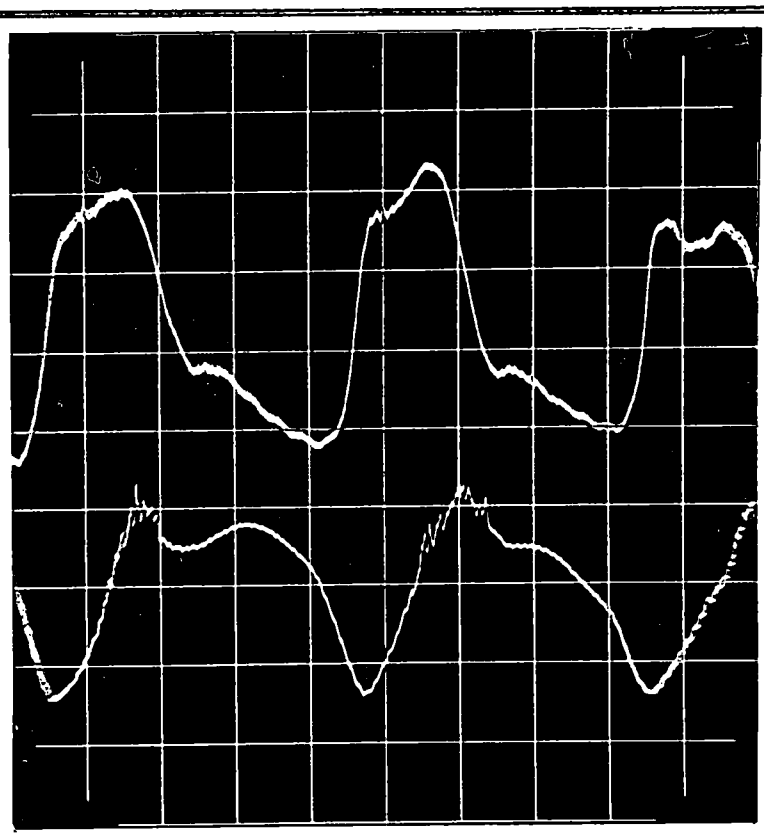

Figure 5.16 Upper trace: combustion chamber pressure. Lower trace: radiation intensity (0C71 mounted above chamber port).

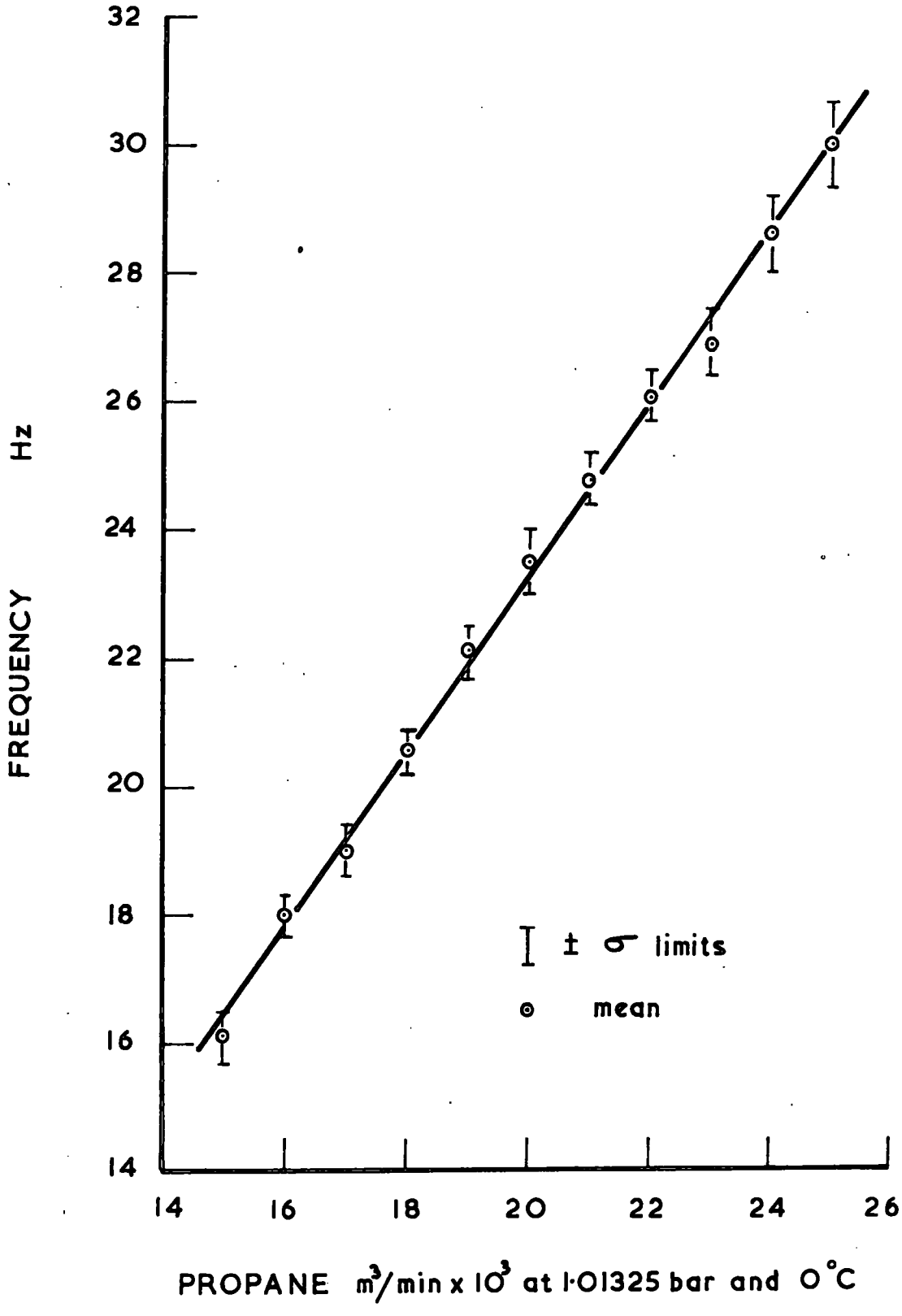

Figure 5·17 Relationship between Fuel Flow and Frequency of Combustion Oscillations.

From this value the Helmholtz frequency under operating conditions was estimated (section 6.2).

5.9 Miscellaneous Results

5.9.1 Heat Transfer

Figure 5.18 shows the variation of heat transfer with pulsation frequency for the wall cooling water and nozzle cooling water.

Heat Flux Density

The maximum heat transfer per unit area for (a) the chamber walls and base, (b) the internal nozzle and (c) the complete combustor, was as follows:-

(a) 68 kW/m^2

(b) 50 kW/m^2

(c) 64 kW/m^2

Variation of heat transfer over chamber walls and base.

Using a thermocouple probe the variation of cooling water temperature down the wall of the combustor was investigated. Most of the temperature rise was found to occur near to the base of the chamber and to obtain some guide as to the distribution of heat transfer over the surface of the combustor the point at which approximately one third of the total temperature rise occurred was determined. This point was approximately 45 mm from the bottom of the combustor wall.

From the above it was calculated that the bottom 25% of

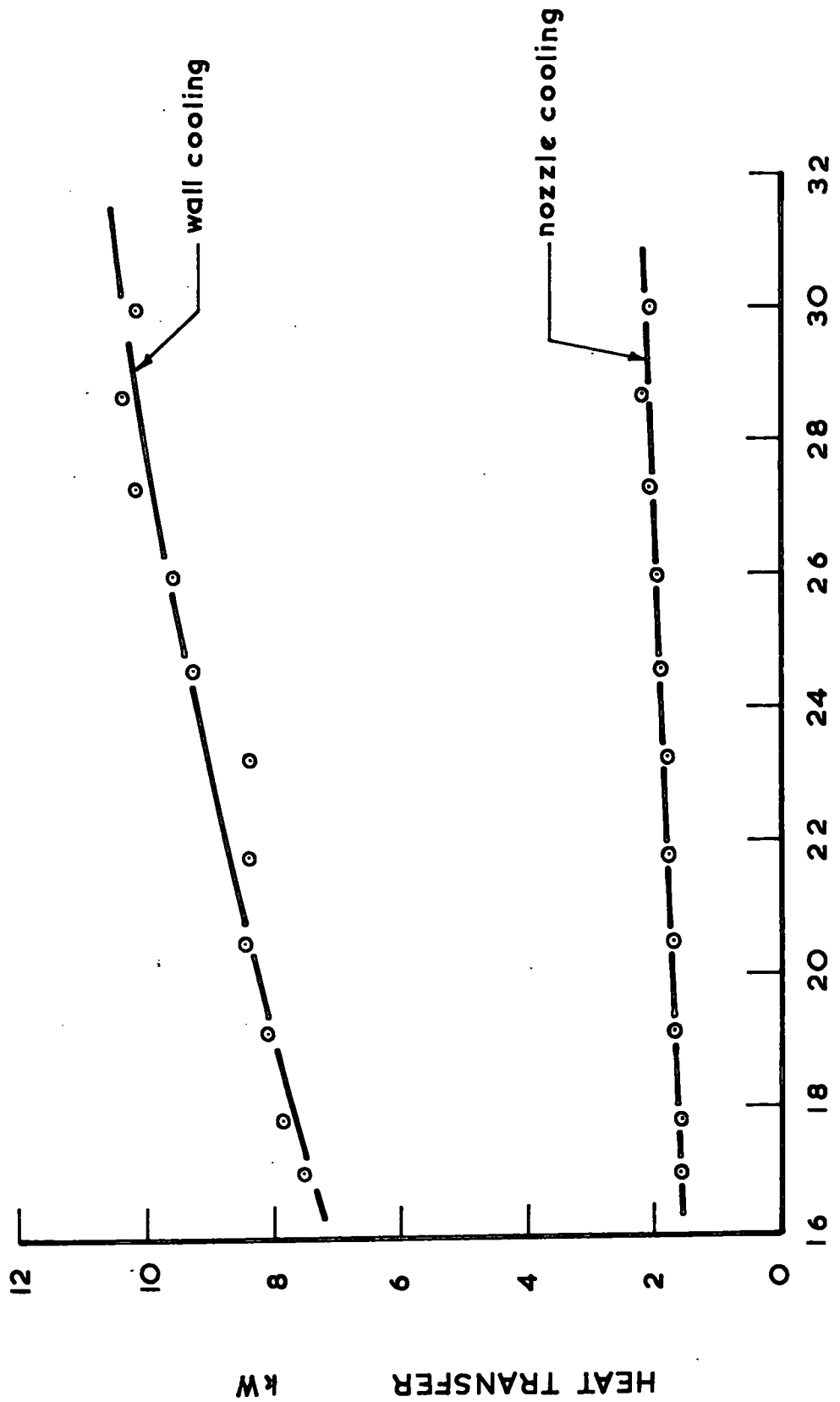

Figure 5·18 Heat transfer to wall and nozzle cooling water.

the combustor surface accounted for almost 70% of the heat transfer.

Table 1. Heat Transfer as Percentage of Energy Released

Propane Flow $m^3/min \times 10^3$	Frequency H_z	% Heat Transfer	Output kW
15	16.5	41.4	21.85
16	17.8	40.8	23.10
18	20.5	39.5	25.65
21	24.6	38.0	29.30
23	27.3	38.4	31.85
24	28.7	38.0	33.00

5.93 Noise Measurements

The spectograms for fuel flows of 0.018 m^3/min and 0.024 m^3/min using standardized weighting 'curve A' are shown in Figure 5.19 while Figure 5.20 shows the background noise (a) with auxiliary equipment (extractor fan, condensate pump etc.) operating and (b) without auxiliary equipment operating.

Figure 5.21

This figure shows the spectograms obtained for a fuel flow of 0.021 m^3/min using (a) an amplifier with a flat response (linear), and (b) an amplifier with a response weighted to standardized weighting 'curve A'.

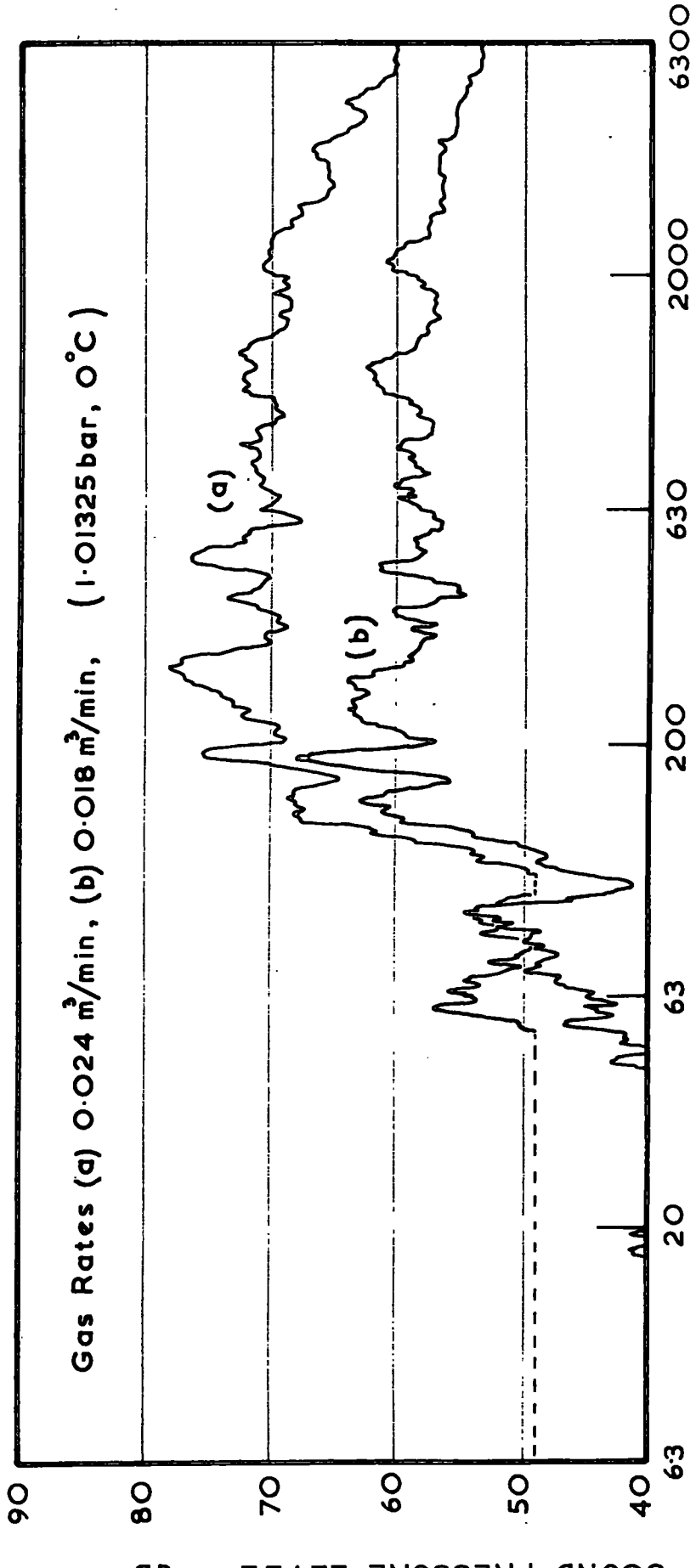

Figure 5·19 Effect of Fuel Flow on Combustor Noise.

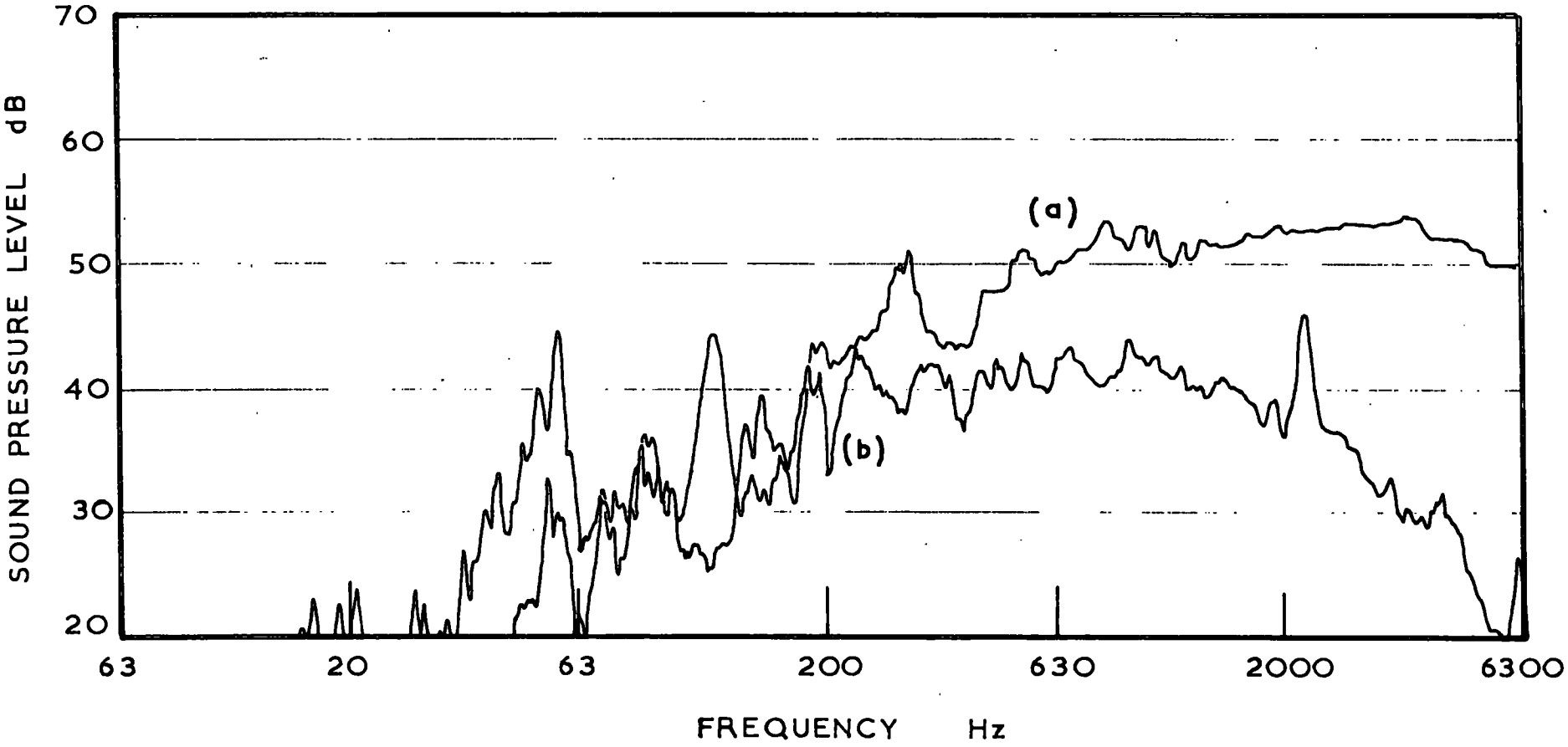

Figure 5·20 Background Noise

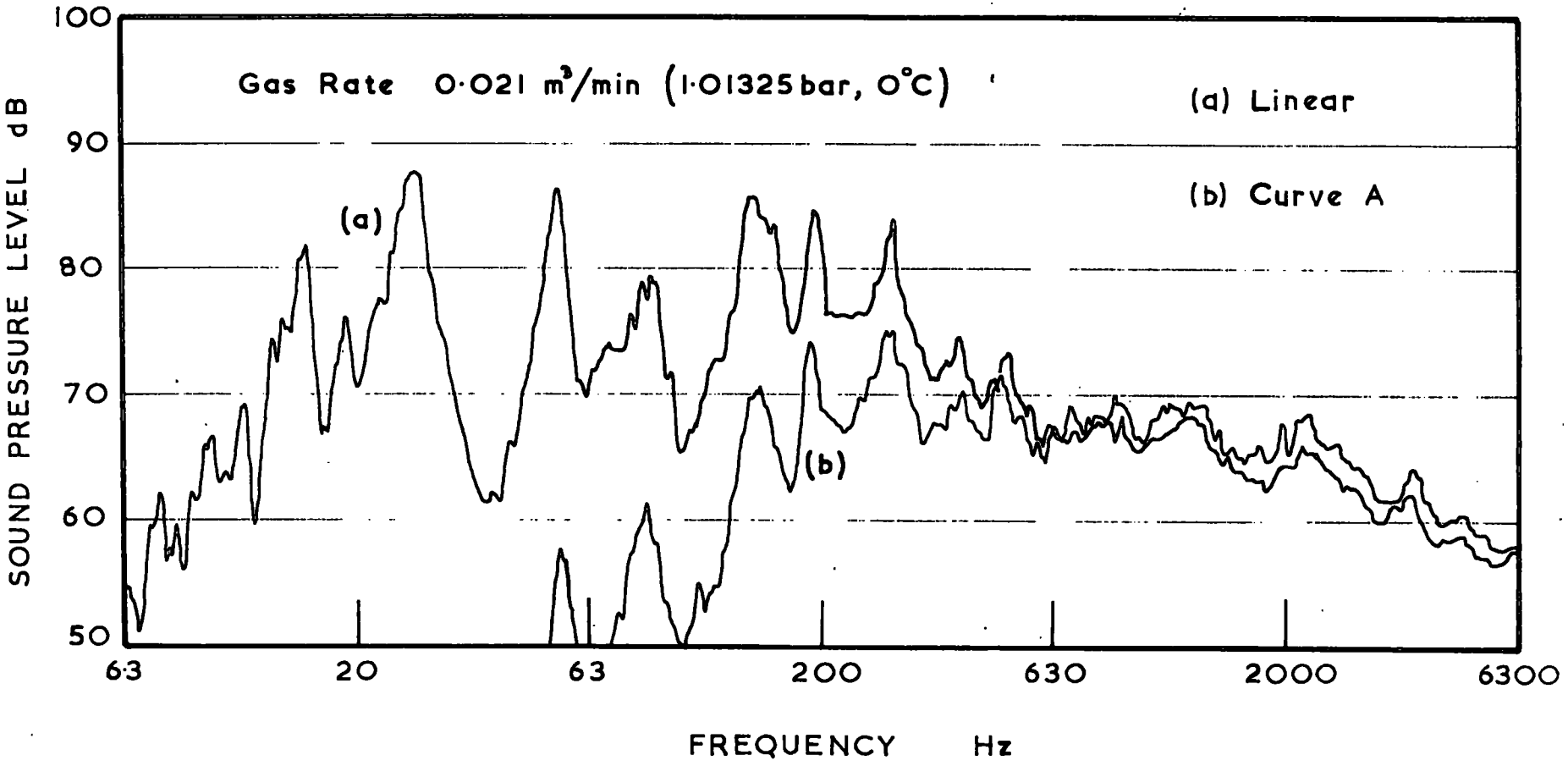

Figure 5·21 Spectrograms of Combustor Noise (a) using linear amplifier, (b) using amplifier with weighting network (Curve A).

5.9.2 Volumetric Efficiency

If the term 'Volumetric Efficiency' is carefully defined, it may be usefully used for design purposes. Volumetric efficiency can be defined as follows:-

$$\text{Volumetric Efficiency} = \frac{\text{Volume}^* \text{ of air inducted per cycle}}{\text{Volume of combustion chamber}}$$

*measured at ambient pressure and temperature.

The volume of the combustion chamber was found by filling the chamber with a measured quantity of water; the volume of combustor III was 0.004 m^3.

The flow of air into the combustion chamber could not be obtained by measurement owing to the fact that some of the air entering the combustor intake was drawn directly into the exhaust pipe by ejector action, without passing through the combustion chamber. To determine volumetric efficiency, therefore, it was necessary to calculate the air flow using values of air/fuel ratio and fuel flow previously determined. The tests for determining air/fuel ratio were quite prolonged and changes in ambient conditions occurred during these tests with the result that the calculated values of volumetric efficiency given in the following table probably include some variation due to changes in ambient conditions.

Table 2

Fuel Flow m^3/min	Frequency H_z	Volumetric Efficiency %
0.015	16.5	10.8
0.016	17.8	10.4
0.018	20.5	10.15
0.021	24.6	9.85
0.023	27.3	9.83
0.024	28.7	9.90

5.9.3 Tests to determine maximum permissible cooling water temperature

These tests at first appeared to substantiate the results of preliminary investigations in that the chamber repeatedly stopped operating when the cooling water inlet temperature exceeded approximately 70°C.

A closer examination of the chamber operation at high cooling water temperatures revealed that water vapour was being injested by the chamber during induction. After measures were taken to stop water vapour entering the chamber the tests were continued and it was then found that the combustor would operate reliably at a cooling water inlet temperature of 85°C. Heat transfer from the cooling system to the surroundings prevented tests at cooling water inlet temperatures higher than 85°C.

5.9.4 Results of observations with a Stroboscope

The small random variations in the frequency of the combustor made it impossible to obtain complete synchronisation of the stroboscope with the combustion cycles. However, synchronisation was good enough to reduce the apparent frequency to less than 1 H_z. The stroboscope did not reveal details of the flame front or the direction of propagation of the flame but it did reveal that at one stage in the cycle combustion was confined to a region close to the base of the chamber.

5.9.5 Solid Deposits on chamber base plate

Figure 5.22 shows the amount of solid deposit that had accumulated on the base plate over an estimated 50 hours of operation. The walls of the combustor were free from such deposits.

This figure also shows the gas nozzle which is in the centre of the base plate and the direction of the gas jet is clearly indicated by the inverted 'V' shaped marking on the surface of the plate.

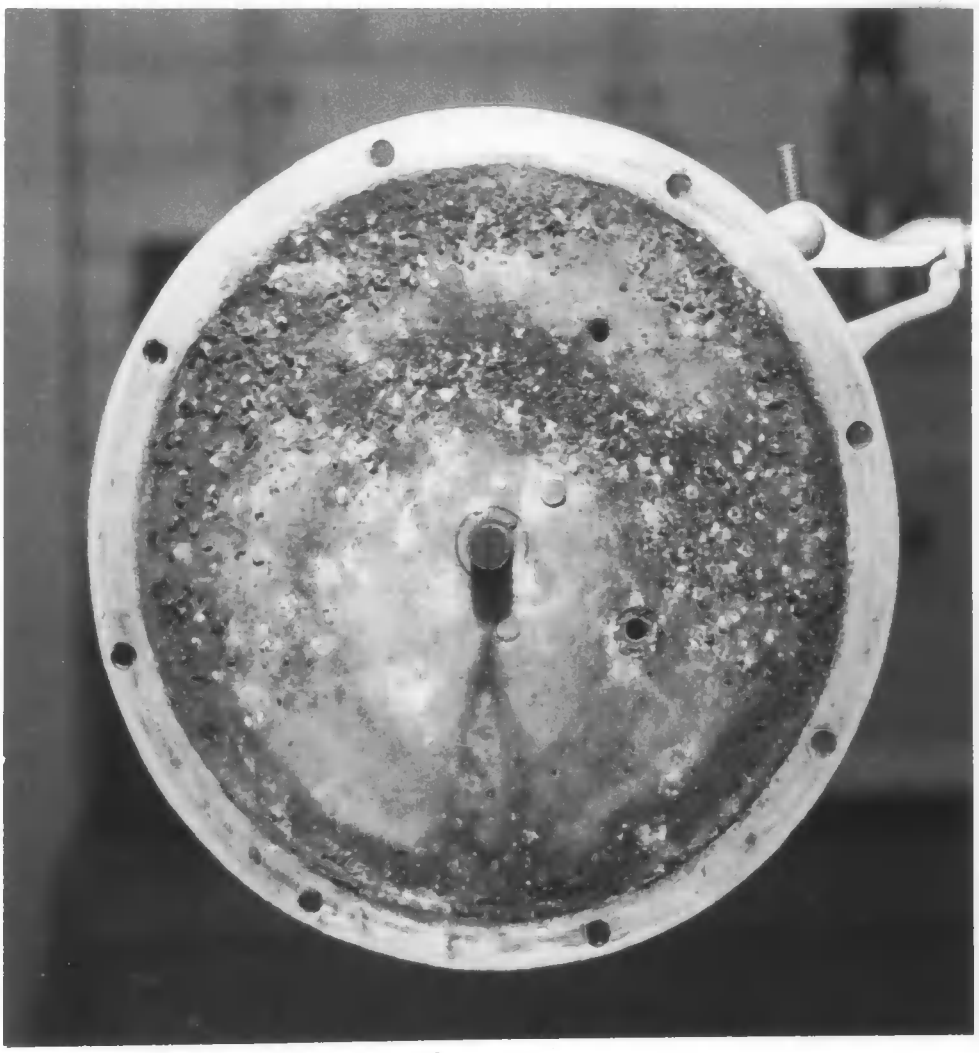

Figure 5.22 Solid deposits on combustor base.

6. THEORETICAL

6.1 Analysis of pressure decay

Porter[8] in his paper "Pulsating Combustion of Liquid Fuel in Partially Closed Vessels" gives the following analysis of the pressure decay part of the exhaust and induction periods:

Assuming uniform conditions throughout the chamber and that the gases are perfect, the equations of conservation of mass and energy for the gases in the chamber, during the pressure-decay period, become

$$\frac{d\rho}{dt} = (\dot{m}_f - \dot{m}_e)/V \qquad (1)$$

$$\frac{dP}{dt} - \frac{\gamma P}{\rho}\frac{d}{dt} = -(\gamma-1)(m_f L + \dot{Q})/V \qquad (2)$$

respectively, where P and ρ are the pressure and density, respectively, of the chamber gases; t denotes time; $\dot{m}_f$ is the fuel vaporization rate; $\dot{m}_e$ is the mass flow rate of gases through the orifice; V is chamber volume; L represents the heat of vaporization of the liquid fuel; $\dot{Q}$ is the total rate of heat loss through the chamber walls; and $\gamma = \frac{Cp}{Cv}$ is the ratio of the specific heats of chamber gases.

Assuming $|(P-Pa)/Pa| \ll 1$, $|(\rho-\bar{\rho})\bar{\rho}| \ll 1$, and neglecting the non-steady acceleration term in the momentum equation, it can be shown that the mass flow rate through the orifice is:-

$$\dot{m}_e \simeq \begin{cases} A_1\left[\rho_a(P-Pa)\right]^{\frac{1}{2}} & \text{for discharge } (P > Pa) \\ A_2\left[\rho_a(Pa-P)\right]^{\frac{1}{2}} & \text{for suction } (P < Pa) \end{cases} \tag{3}$$

where the subscript 'a' refers to ambient air, $\bar{\rho}$ is some constant average density in the chamber, $A_1 = A(2\bar{\rho}/\rho_a)^{\frac{1}{2}}$, and $A_2 = A(2)^{\frac{1}{2}}$ are modified orifice areas for discharge and suction respectively, and A is the actual orifice area. Letting P = P max. at time t = 0 (corresponding to the beginning of pressure decay), and assuming that the fuel vaporization rate $\dot{m}_f$ and heat transfer $\dot{Q}$ are constant, equations (1), (2) and (3) may be combined and integrated* to yield

$$(y_1,\text{max.}-y_1) - \text{Log}\left[(1+y_1,\text{max.})/(1+y_1)\right] = t_1,$$

$$\text{for } 0 \leqslant t \leqslant t_o \tag{5}$$

and

$$\text{Log}\left[1/(1-y_2)\right] - y_2 = t_2, \text{ for } t_o \leqslant t \leqslant \tau^{**} \tag{6}$$

where

$$y_{1,2} = \left\{ \frac{A_{1,2}(Pa\,\rho_a)^{\frac{1}{2}}}{(\gamma-1)(\rho_a/\gamma Pa)(\dot{m}_f L+\dot{Q}) - \dot{m}_f} \right\} \left[\frac{|P-Pa|}{Pa} \right]^{\frac{1}{2}} \quad \text{and}$$

$$t_{1,2} = \left\{ \frac{\gamma(A_{1,2})^2\, Pa}{2V\left[(\gamma-1)(\rho_a/\gamma Pa)(\dot{m}_f L+\dot{Q})-\dot{m}_f\right]} \right\} t \tag{7}$$

* By combining equations (1), (2) and (3) for the discharge (exhaust) period the following equation is obtained.

$$-A_1\left[\rho_a(P-Pa)\right]^{\frac{1}{2}} = \frac{V}{\gamma}\frac{\rho}{\bar{P}}\frac{dP}{dt} + \left[\frac{\rho}{\bar{P}}\left(\frac{\gamma-1}{\gamma}\right)(\dot{m}_f L+\dot{Q})-\dot{m}_f\right] \tag{4}$$

This equation can only be integrated to obtain P = Q(t)

providing ρ can be eliminated from the equation. Porter apparently assumed $\frac{\rho}{P} = \frac{\rho a}{Pa}$ although this is not stated in his paper. By putting $\frac{\rho}{P} = \frac{\rho a}{Pa}$ equation (4) can be integrated to yield equations (5), (6) and (7).

** The statement $t_o \leqslant t \leqslant \tau$ is confusing in that by putting P = Pa (i.e. start of induction) the value t = 0 is obtained. The explanation here is that the induction and exhaust periods must be considered separately and therefore for the induction period the time t is counted from the start of the induction period and not from the start of the pressure decay part of the exhaust period as indicated by $t_o \leqslant t \leqslant \tau$.

Application of equations (5), (6) and (7) to a gas-fired combustor.

In the case of a gaseous fuel the term $\dot{m}_f L$ in the denominators of the expressions for $y_{1,2}$ and $t_{1,2}$ is zero.

Hence,

$$y_{1,2} = \frac{A_{1,2}(Pa\rho a)^{\frac{1}{2}}}{\left[\left(\frac{\gamma-1}{\gamma}\right)\frac{\rho a}{Pa}\dot{Q} - \dot{m}_f\right]} \cdot \left(\left|\frac{P-Pa}{Pa}\right|\right)^{\frac{1}{2}}$$

$$\bar{t}_{1,2} = \frac{\gamma (A_{1,2})^2 Pa}{2V\left[\left(\frac{\gamma-1}{\gamma}\right)\frac{\rho a}{Pa}\dot{Q} - \dot{m}_f\right]} \cdot t$$

$$\bar{t}_1 = (y_{1,max} - y_1) - \text{Log}\left[(1+y_{1,max})/(1+y_1)\right]$$

$$\bar{t}_2 = \text{Log}\left[1/(1-y_2)\right] - y_2$$

Theoretical Pressure Decay for a Gas Rate of 21 x 10^{-3} m^3/min.

Te = 1370 K; calculated value of exhaust temperature.

$\bar{P}$ = 102.265 kN/m^2; mean pressure during exhaust.

A_1 = 3.25 x 10^{-4} m^2.

$A_2 = 7.18 \times 10^{-4} m^2$.

$Pa = 100.6 \text{ kN/m}^2$.

$Ta = 291 \text{ K}$

$\rho_a = 1.205 \text{ kg/m}^3$.

$\gamma = 1.285$; calculated from exhaust gas analysis.

$V = 4 \times 10^{-3} \text{ m}^3$.

$\dot{Q} = 11.15 \times 10^3 \text{ J/s}$.

$\dot{m}_f = 0.7 \times 10^{-3} \text{ kg/s}$.

$$\left(\frac{\gamma-1}{\gamma}\right)\frac{\rho_a}{Pa}\dot{Q} - \dot{m}_f = \frac{0.285}{1.285} \times \frac{1.205}{100.6 \times 10^3} \times 11.15 \times 10^3 - 0.7 \times 10^{-3}$$

$$= \underline{28.9 \text{ kg/s}}$$

Exhaust Period

$$y_1 = \frac{3.25 \times 10^{-4} \ (100.6 \times 10^3 \times 1.205)^{\frac{1}{2}}}{36.3 \times 10^{-3}} \cdot \left(\frac{|P-Pa|}{Pa}\right)^{\frac{1}{2}}$$

$$y_1 = 3.91\left(\frac{|P-Pa|}{Pa}\right)^{\frac{1}{2}}$$

$$\bar{t}_1 = \frac{1.285 \times 3.25^2 \times 10^{-8} \times 100.6 \times 10^3}{2 \times 4 \times 10^{-3} \times 28.9 \times 10^{-3}} \cdot t$$

$$\bar{t}_1 = 59.1 \ t$$

$Pmax = 3.03 \times 10^3 \text{ N/m}^2$ gauge

$$y_1,max = 3.91 \times \left(\frac{3.03}{100.6}\right)^{\frac{1}{2}} = 0.678$$

$$\therefore \ \bar{t}_1 = (0.678 - y_1) - Log\left(\frac{1.678}{1+y_1}\right)$$

$P = 3.03 \text{ kN/m}^2 g \ t = 0$

$P = 2\ kN/m^2g \quad t = 0.815\ ms$

$P = 1\ kN/m^2g \quad t = 1.71\ ms$

$P = 0\ kN/m^2g \quad t = 2.71\ ms$

Induction Period

$$\bar{t}_2 = \text{Log}[1/(1-y_2)] - y_2$$

$$\text{and } \bar{t}_2 = \frac{1.38 \times 7.18^2 \times 10^{-8} \times 100.6 \times 10^3}{2 \times 4 \times 10^{-3} \times 36.3 \times 10^{-3}} \cdot t$$

$$\bar{t}_2 = 247\ t$$

$$y_2 = \frac{7.12 \times 10^{-4}\ (100.6 \times 10^3 \times 1.21)^{\frac{1}{2}}}{36.3 \times 10^{-3}} \cdot \left(\left| \frac{P-Pa}{Pa} \right| \right)^{\frac{1}{2}}$$

$$y_2 = 6.93 \cdot \left(\left| \frac{P-Pa}{Pa} \right| \right)^{\frac{1}{2}}$$

P	$= -0.5\ kN/m^2g$	$t = 0.74$ ms
P	$= -1.0\ kN/m^2g$	$t = 1.94$ ms
P	$= -1.5\ kN/m^2g$	$t = 4.19$ ms
P	$= -1.9\ kN/m^2g$	$t = 8.77$ ms
Pmin.	$= -2.09\ kN/m^2g$	$t = \infty$ ms

The theoretical pressure decay curve is shown in Figure 6.1.

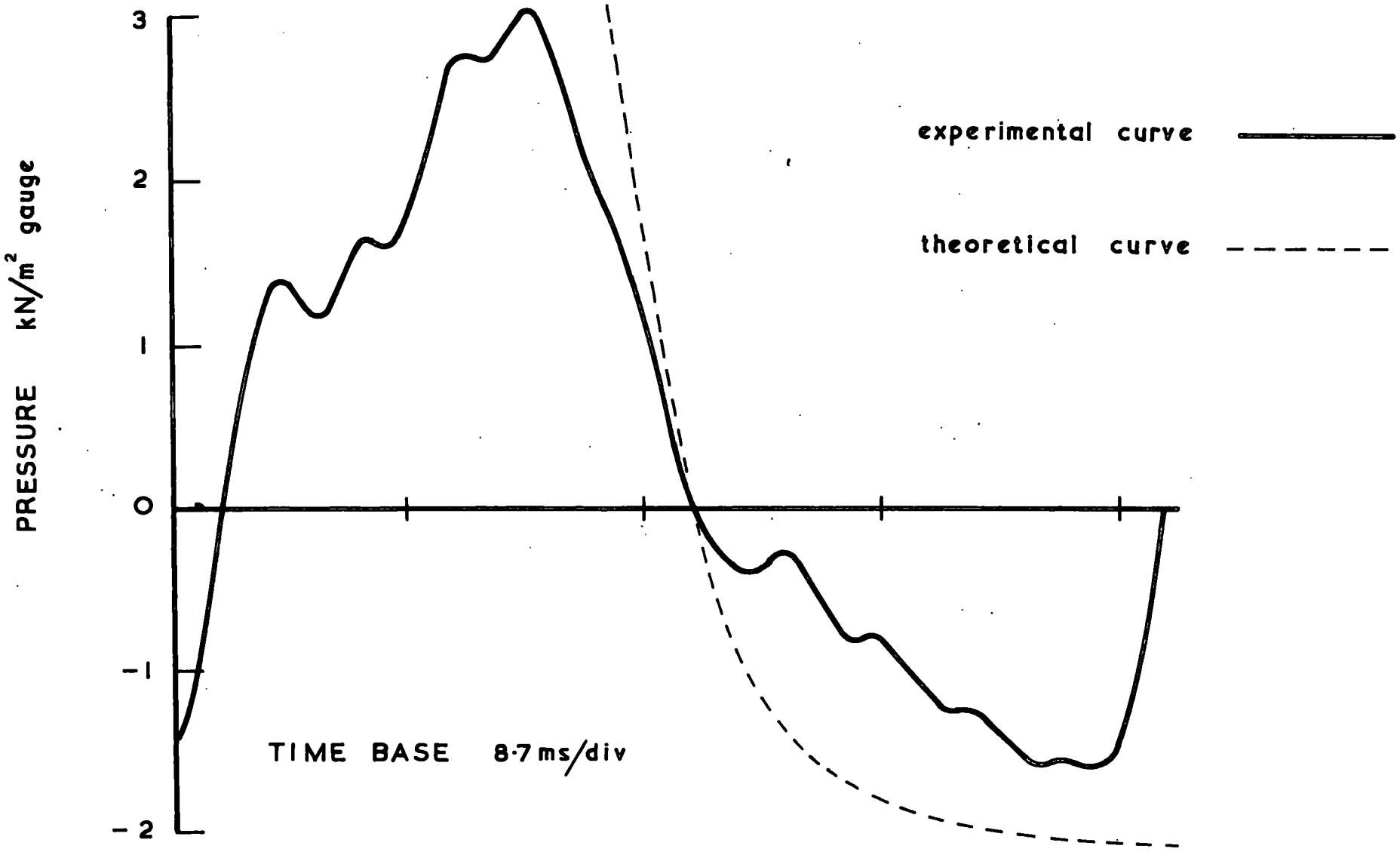

Figure 6·1. Experimental and Theoretical Pressure/Time Curves.

6.2 Helmholtz Frequency of Combustion Chamber

The frequency of a Helmholtz resonator can be determined by considering the motion of a small plug of gas in the neck of the resonator.

Let S be the cross-sectional area of the plug

x be the displacement of the plug

dP be the difference in pressure across the plug

ℓ be the length of the plug

Then the force acting on the plug = $dP\ S$ (1)

Since the external face of the plug is subject to constant pressure (atmospheric pressure) it follows that dP is the increase in pressure in the combustion chamber caused by the compression of the gas due to the displacement of the plug.

If the volume displacement of the plug is dV and the chamber volume is V then;

$dP = -K \frac{dV}{V}$ where K is the coefficient of compressibility of the gas in the chamber.

Now for a gas $K = C^2\rho$ where C is the velocity of sound in, and ρ is the density, of the gas in the chamber

hence $dP = -C^2\rho \frac{dV}{V}$ (2)

From (1) and (2) we have:

Force acting on plug = $-C^2\rho \frac{dV}{V} S$

but $dV = Sx$

$\therefore$ Force acting on plug = $\frac{-c^2\rho S^2}{V} \cdot x$

and the mass of the plug = $\rho' \ell S$ where ρ' is the density of the gas forming the plug.

$$\ddot{x} = \frac{-c^2\rho S^2}{\ell\rho' SV} x = \frac{-c^2\rho S}{\ell\rho' V} x$$

$$\therefore \ddot{x} + \frac{c^2\rho S}{\ell\rho' V} \cdot x = 0 \qquad (3)$$

The plug therefore moves with S.H.M. and the frequency n is given by

$$n = \frac{1}{2\pi}\left(\frac{c^2\rho S}{\ell\rho' V}\right)^{\frac{1}{2}} \qquad (4)$$

Now Rayleigh[11] has shown that for a circular aperture in a thin wall the effective length of the plug is given by,

$\ell = \frac{S}{d}$ where d is the diameter of the aperture

Also, for a gas $c^2 = \gamma RT$

Hence equation (4) becomes:

$$n = \frac{1}{2\pi}\left(\gamma RT \frac{\rho}{\rho'} \frac{d}{V}\right)^{\frac{1}{2}}$$

$\frac{\rho}{\rho'} = \frac{T'}{T}$ where T' is the temperature of the gas forming in the plug.

$$\therefore n = \frac{1}{2\pi}\left(\frac{\gamma RT'd}{V}\right)^{\frac{1}{2}}$$

For a fuel flow of 0.021 m^3/min we have:

T' = 1370 K

γ = 1.285)

R = 0.299 kJ/kg K) based on exhaust gas analysis

$$d = 25.4 \times 10^{-3} \text{ m}$$

$$V = 4 \times 10^{-3} \text{ m}^3$$

$$n = \frac{1}{2\pi}\left(\frac{1.285 \times 0.299 \times 10^3 \times 1370 \times 25.4 \times 10^{-3}}{4 \times 10^{-3}}\right)^{\frac{1}{2}}$$

$$n = 291 \text{ H}_z$$

Under ambient conditions of 291 K and 760 mm Hg the Helmholtz frequency was determined experimentally and found to be 110 H_z.

$n = 110 \text{ H}_z$ at 291 K and 760 mm Hg corresponds to

$n = 240 \text{ H}_z$ at working conditions for a fuel flow of 0.021 m^3/min.

Frequency from Pressure/Time record - Figure 6.1

Assuming that the small perturbations on the pressure record are caused by small amplitude Helmholtz type oscillations, the frequency of such oscillations is

$n = 306 \text{ H}_z$

7. DISCUSSION

7.1 Combustor Design

The internal geometry of the chamber used in this investigation was, for all practical purposes, identical with a design of Reynst's. In Reynst's design however details such as the position of the sparking plug and the size and precise position of the gas nozzle were not given. A considerable amount of time was spent in determining the above details in order to secure proper operation of the combustor. From this work it was established that with the sparking plug situated in the wall near to the top of the chamber and with the gas entering close to the base in a radial direction from a single nozzle, the chamber would operate.

Once the correct operating conditions had been determined the "start up" and subsequent operation of the combustor was reliable providing condensate was not permitted to collect in the chamber and so flood the gas nozzle. In a practical combustor, therefore, it would probably be necessary to have the chamber inverted to allow the condensate to drain away.

With the gas entering the chamber directly (instead of being inducted with the air) the efficiency was low, being only 87.5% maximum. This low efficiency is in agreement with Reynst's findings for direct injection but it is hoped that by further development work on the gas nozzle arrange-

ment the efficiency can be increased to an acceptable level.

In designing a combustor with a specified output the "volumetric efficiency" is an important design parameter. The volumetric efficiency of the combustor investigated was found to be within the range 9.8 to 10.8%; Reynst quoted a value of 13% for his combustor. For design purposes therefore it would be reasonable to use a value of 10%.

Two other important design parameters are (i) chamber port diameter/chamber length, ratio and (ii) frequency - volume - fuel flow relationship for various values of (i). The above parameters could form the basis of a further investigation.

7.2 Heat Transfer

Heat transfer measurements show that most of the heat transfer occurs in the lower part of the combustor. This fact is also corroborated by the mean isotherm pattern of Figure 5.6.

Heat transfer to cooling water accounts for approximately 40% of the total energy release, the percentage decreasing slightly with increasing frequency.

The maximum value recorded for the average heat flux density over the entire internal surface of the combustor was 64 kW/m^2. For the bottom 25% of the combustor surface only, the corresponding value was 180 kW/m^2 which compares favourably with a value of 168 kW/m^2 obtained by Hanby[12] for a tubular propane-fired combustor under pulsating operation.

7.3 Combustion Intensity and Noise Level

The combustor was found to be reliable in operation up to a combustion intensity of approximately 8.25 MW/m^3. At intensities higher than this the combustor would frequently cut out after only a few minutes operation. The value of 8.25 MW/m^3 is less than half the intensity of combustion Reynst quotes for the combustor shown in Figure 3.2 which burned liquid fuel and operated in resonance with its exhaust pipe.

Operating a combustor under resonant conditions would no doubt improve its performance in terms of combustion intensity but it would also aggravate the serious problem of combustor noise. The author is of the opinion therefore that it is better to operate the combustor out of resonance with its exhaust pipe thereby reducing the noise level even if this does mean a reduction in combustion intensity.

From sound pressure measurements taken at a distance of 1 m from the chamber port, the overall sound pressure level at maximum fuel flow was calculated to be 83 dB (ref 2×10^{-5} N/m^2). Gellar[1] et al quotes a value of 93 dB for a pulsating-combustion heater of the Helmholtz type having a rated output similar to that of the author's combustor and Reay[3] quotes a value of 118 dB for a 53 kW unit. In comparison therefore the Reynst type combustor operating under non-resonant conditions is relatively quiet.

7.4 Frequency of Combustion Oscillations

Pulsation frequency was always much lower than the Helmholtz frequency of the combustion chamber, e.g. a pulsation frequency of 25 H_z represents only 8% of the corresponding Helmholtz frequency. This result, which is in general agreement with Porter's findings on a liquid fueled Reynst type combustor confirms that the instability is not of the acoustic type.

The frequency/fuel flow tests revealed that for the Reynst type of combustor operating on direct gas injection, there is an almost linear relationship between frequency and fuel flow (Figure 5.17). This result was not unexpected since in his papers, Reynst claims that for a gas-fired combustor, the frequency (up to resonance) is proportional to fuel flow, he does not however give any data to support this.

7.5 Chamber Pressure as a Function of Time

(i) Experimental Pressure/Time diagrams

The diagram shown in Figure 6.1 is typical of the pressure/time diagrams recorded using the strain gauge pressure transducer. An interesting feature on the diagram is the small but regular fluctuations in pressure that are superimposed on the main variation of pressure with time. At first it was thought that these perturbations might be due to resonance of the tube and cavity, between the dia-

phram of the pressure transducer and the combustion chamber, however it was soon established that the natural frequency of the transducer system was much higher than the frequency of the perturbations on the pressure trace. Another possible explanation was that the perturbations were Helmholtz type oscillations superimposed on the flow into and out of the combustion chamber. To check this, the Helmholtz frequency of the combustion chamber was determined, and compared with the frequency of the perturbations. The agreement between the frequency of the Helmholtz oscillations and of the perturbations was very close (Page 83) and suggests that this latter explanation is correct.

From Figure 6.1 it can be seen that the rate of pressure decay is greater during the latter part of the exhaust period than during the induction period. The reason for this becomes clear when one considers that during the exhaust period the loss of gas from the chamber augments the effect of cooling of the gas in reducing chamber pressure, whilst during the induction period, the flow of gas into the chamber tends to counteract the pressure drop due to cooling.

(ii) Amplitude of Fluctuating Chamber Pressure

Both the positive and negative peak pressures were found to increase with increasing fuel flow (or frequency). However, the positive peak pressure showed a tendency to level off as the fuel flow approached

the values at which the combustor became unreliable in operation, this effect can be seen in Figure 5.4 . The amplitude of the chamber pressure was much lower than had been expected, the maximum positive value being only 4.2 kN/m^2 gauge.

(iii) Theoretical Pressure Decay Curve

In Figure 6.1 the theoretical pressure decay curve obtained by modifying Porter's analysis for application to a gas-fired combustor is shown superimposed on a typical experimental curve. The rather poor agreement between the two curves is an indication that some of the assumptions made in the analysis are not valid. Two assumptions viz. (a) zero chemical reaction during pressure decay, and (b) constant heat transfer almost certainly account for the major part of the discrepancy between the two curves.

It would appear, therefore, that although Porter's analysis goes some way towards describing the pressure decay process, a more rigorous treatment is required before quantitative agreement between theory and experiment can be reached.

7.6 Flame Speed - Use of Ion Probes

The use of ion probes to detect the flame front did not present many problems but the aim of using these probes to determine flame speed was not realised, due to the difficulty of determining the direction of flame propogation.

Observations with the stroboscope disc did occasionally reveal a flame movement in an approximately vertical direction but it was not possible to determine whether the movement was vertically upwards or vice versa. For a vertically upwards propogating flame the speed between sections 7 and 3 was estimated to be 3.8 m/s and for a vertically downwards propogating flame 18.7 m/s (from the record shown in Figure 5.11).

The records obtained with the ion probes indicate that the probes respond to hot gas alone. This is shown in Figures 5.12 and 5.13 which are for sections above the combustion zone.

7.7 Ignition of Each Charge

Although no definite conclusion has been reached regarding the source of ignition of each charge, from observations with the stroboscope disc the author has formed the opinion that the process is one of fluctuating combustion rather than intermittent combustion.

7.8 Information from Radiation/Time Records

The simultaneous radiation/time and pressure/time record (Figure 5.16) shows that during the first stage of the pressure decay period, the radiation level is still quite high and it is probable, therefore, that a considerable amount of combustion occurs during this period. The differences between the record obtained with the phototransistor mounted above the chamber port and the record obtained with it mounted in the window of the chamber can be accounted for by the fact

that its field of view in the latter position was restricted to a relatively small part of the combustion zone (the space between the internal nozzle and the chamber floor), whereas when mounted above the chamber port, the phototransistor could 'see' practically all of the combustion zone. Figures 5.15 and 5.16 also show that the radiation peak occurs later than the pressure peak.

Records of the type shown in Figure 5.14 were obtained in an attempt to establish whether or not a flame was always present in the combustion chamber during normal operation. However the response of the phototransistor to visible radiation from the flame was later shown to be almost nil and hence the fact that the radiation level remains above the zero line cannot be taken to be evidence of a flame in the combustion chamber.

8. CONCLUSIONS

From this investigation it has been concluded that the combustion instability in a Reynst type combustor is of the fluid-dynamic type of combustion chamber instability. In arriving at this conclusion, two other types of instability had to be taken into account, these were (i) system instability and (ii) acoustic instability. System instability was eventually discounted on the grounds that the combustor could be operated at gas nozzle inlet pressures high enough to produce choked flow in the gas nozzle, and acoustic instability on the grounds that the operating frequency was always much lower than the Helmholtz frequency and could be varied over a considerable range by regulating the fuel supply.

The theoretical analysis of the induction process did not reach quantitative agreement with the experimental results. However, the quantitative agreement was sufficiently good to show that heat transfer, and not wave action, is the important factor in the process. This confirms Reynst's claim that the induction process is one of "thermal breathing".

Combustor noise was lower than had been expected, the highest overall sound pressure level being only 83 dB (ref. 1 dB = 2×10^{-5} N/m^2). This fairly low noise level was probably due to the combustor being operated out of resonance with its exhaust pipe. Work by other investigators on the silencing of pulse combustors indicates that a sound pressure level of 83 dB could be reduced to 50-60 dB by

means of insulation and exhaust silencing.

Combustion efficiency was found to be lower than would normally be acceptable, but this could possibly be improved by modifications to the gas nozzle or by operating the combustor on an inducted gas/air mixture instead of direct gas supply. Operation on an inducted gas/air mixture would, however, create problems in automatic control since a direct gas supply would still be required for starting the combustor.

Regarding combustor design, some information has been obtained by this investigation, such as the size and position of the gas nozzle, gas pressure, position of sparking plug etc., but a considerable amount of work still remains to be carried out before cut and try methods can be eliminated.

On the theoretical side, a more rigorous treatment of the operating cycle is required and a theoretical analysis of the relationship between frequency - fuel flow and chamber dimensions, together with a method of predicting the frequency - fuel flow operating range of a combustor would be of value to the designer.

G. Everson

May, 1971.

9. REFERENCES AND BIBLIOGRAPHY

References

1. Geller L.B., Lee G.K. and Mitchell E.R.
High intensity combustion for pulsating and sonic heating systems.
ASHRAE Journal, September 1964.

2. Francis W.E., Hoggarth M.L. and Reay D.
A study of Gas-Fired Pulsating Combustors for Industrial Applications.
The Gas Council Research Communication GC91.

3. Reay D.
The Termal Efficiency, Silencing and Practicability of Gas-Fired Industrial Pulsating Combustors.
The Gas Council External Report No. 102.

4. Alebon J., Lee G.K. and Geller L.B.
A Pulsating Combustion System for Space Heating.
Paper presented at First Conference on Fuel Technology in Canada, Montreal, May 21-23 1963.

5. Huber L.
Mit Schwingfeuer betriebene Heizanlagen fur Nutzfahrzeuge.
Auto Tech Zeit 1951, Volume 53.

6. Sampath P.
Investigations on a Helmholtz type Pulse Combustor.
U.S.G.R.D.R. No. PB-173804.

7. Thring M.W. editor.
Pulsating Combustion : the collected works of F.H. Reynst.
Pergamon Press 1961.

8. Porter J.W.
Pulsating Combustion of Liquid Fuel in Partially Closed Vessels.
Combustion and Flame 11, 501 (1967).

9. Putman A.A.
General Considerations of Combustion Oscillations.
Chapter F in Non-steady Flame Propagation,
G.H. Markstein, Ed., Pergamon Press 1964.

10. Barrére M. and Williams F.A.
Comparison of Combustion Instabilities found in various types of Combustion Chambers.
Twelfth Symposium (International) on Combustion, P. 169.

11. Rayleigh
Theory of Sound.

Bibliography

1. Thring M.W.
Combustion Oscillations in Industrial Combustion Chambers.
Twelfth Symposium (International) on Combustion, P. 163.

2. Foa J.V.
Elements of Flight Propulsion.
Wiley 1960.

3. Blackshear P.L., Jr.,
Driving Standing Waves by Heat Addition.
Fourth Symposium (International) on Combustion, P. 553.

4. Hanby V.I.
Convective Heat Transfer in a Gas-Fired Pulsating Combustor.
ASME Journal of Engineering Power 91 : 48-52 Jan 1969.

5. Hanby V.I. and Brown D.J.
50 lb/h Pulsating Combustor for Pulverized Coal.
Journal of the Institute of Fuel.
Volume 41 No. 334, Nov. 1968, P. 423-6.

6. Putnam A.A. and Dennis W.R.
Burner Oscillations of the Gauze-Tone Type.
The Journal of the Acoustical Society of America
Volume 26, No. 5, September 1954.

7. Markstein G.H.
Non Steady Flame Propagation
Pergamon Press - New York - 1964.

8. Mosely P.E. and Porter J.W.
Helmholtz Oscillations in Pulsating-Combustion Chambers.
The Journal of the Acoustical Society of America.
Volume 46 No. 1 (Part 2) P. 262, 1969.

9. Bannister F.K. and Mucklow C.F.
Wave Action Following Sudden Release of Compressed Gas from a Cylinder.
Proc. I. Mech. E. Vol 159, 1948. P. 269.

10. Dekker B.E.L. and Chang Y.F.
Transient Effects in the Discharge of Compressed Air From a Cylinder Through an Orifice.
ASME Journal of Basic Engineering. September 1968 P. 333.

11. Duclos D.P. and Grounds W.M.
Flame Ionization Detector.
Review of Scientific Instruments.
Volume 27, February 1956, P. 111-112.

12. Heys T.M.
A Rectification Flame Detection Probe with Inbuilt Earthed Area.
Gas Council External Report ER 68.

13. Markstein G.H. and Somers L.M.
Cellular Flame Structure and Vibratory Flame Movement in N-Butane-Methane Mixtures.
Fourth Sumposium (International) on Combustion, P. 527.
The above paper gives details of the use of ion probes for measuring flame speed.

10. APPENDIX

Information relating to exhaust gas analysis using Shandon UK3 Gas Chromatograph

Detector	Thermal Conductivity
Detector Current	140 mA
Column	1m x 4.5 mm force
Packing	60-80 mesh Molecular Sieve
Carrier Gas	Helium
Carrier Gas Flow	60 cm/min
Oven Temperature	$70^{o}C$
Sample Size	0.8 cm

Recorder

Sensitivity	10 mv F.S. for O, N and CH
	1 mv F.S. for CO
Paper Speed	1 cm/min

Calibration Mixture:-

Volumetric Analysis	O_2	Ar	CO	CO_2	N_2
%	4.82	0.22	2.98	9.03	82.95

Information relating to exhaust gas analysis using Pye Series 104 Chromatograph

Detectors (two)		Thermal Conductivity
Detector Current		95 mA
Carrier Gas		Argon
Carrier Gas Flow Rate		60 cm/min
Oven Temperature		$50^{o}C$
Columns	1.	Molecular sieve 80-100 mesh
		1.5 m x 4 mm bore
	2.	Silica Gel 80-100 mesh
		1.5 m x 4 mm bore
Sample Size		0.5 cm for Molecular Sieve
		1.0 cm for Silica Gel
Recorder		Honeywell Strip Chart Recorder
Paper Speed		18 in/hr
Sensitivity		Recorder 1 mv F.S. chromatograph
		2:1 Attenuation for CO and
		20:1 for H

Calibration Mixture:-

Volumetric Analysis	O_2	Ar	CO	CO_2	N_2
%	4.88	0.22	2.98	9.03	82.95

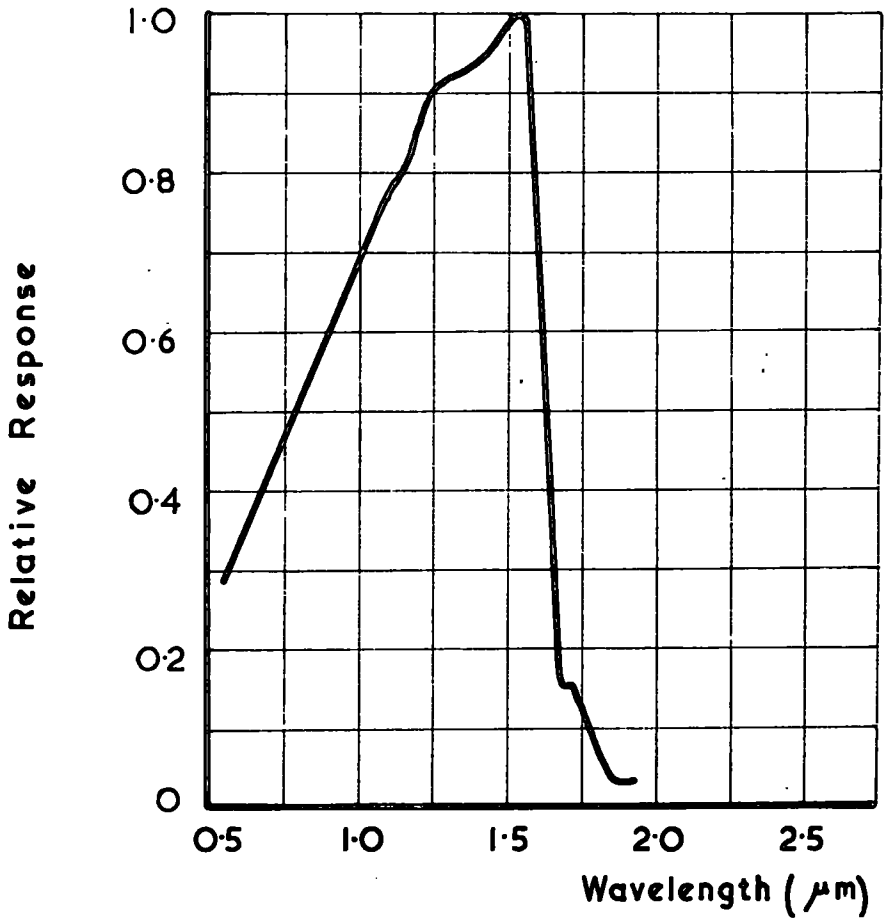

Figure 10·1 Spectral Response of BXP25.

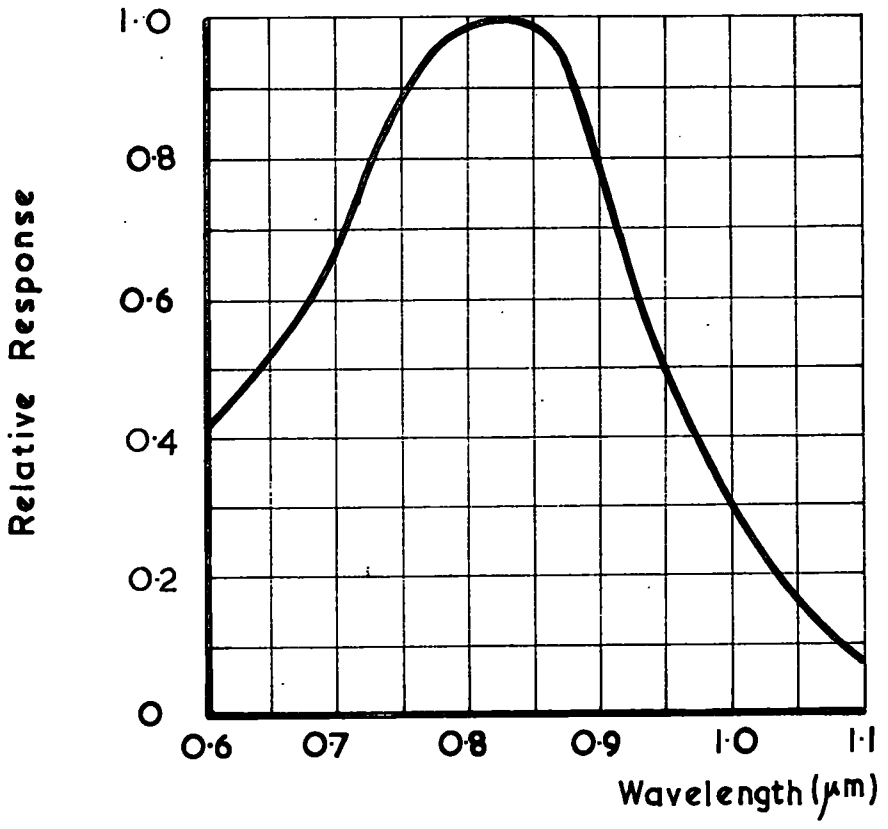

Figure 10·2 Spectral Response of OCP 71